Aupouri Aquifer Groundwater Model

Factual Technical Report - Modelling

WILLIAMSON WATER & LAND ADVISORY
WWLA0184 | 3

5 February 2020

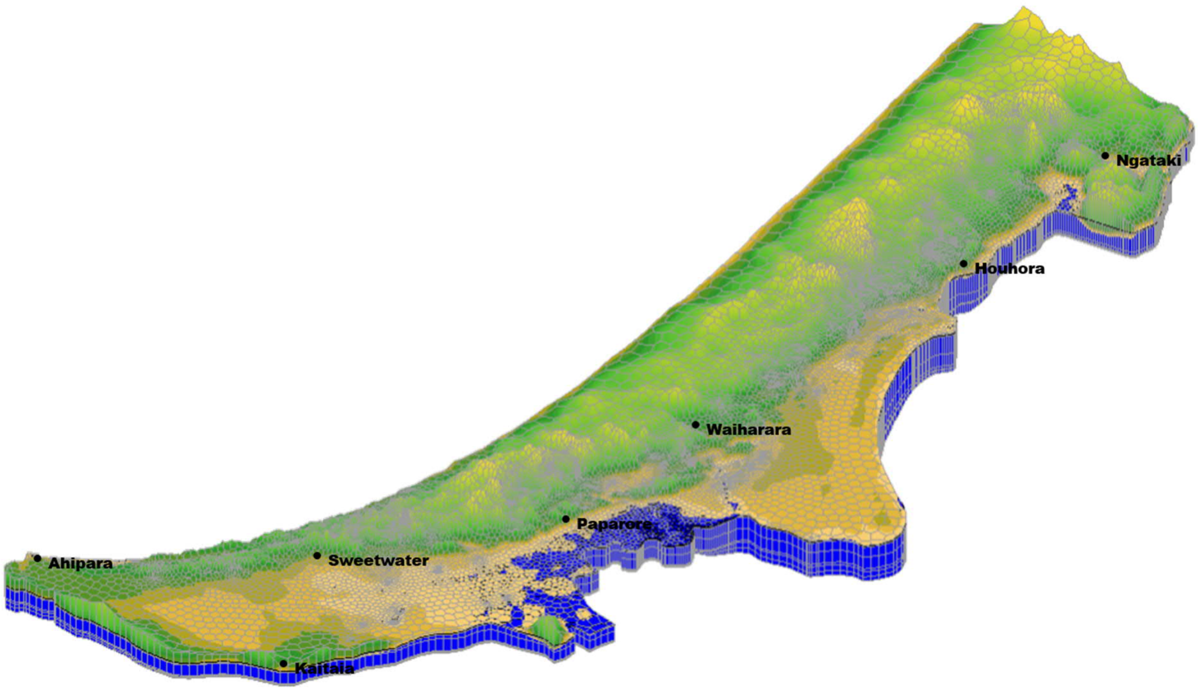

Aupouri Aquifer Groundwater Model

Project no: WWLA0184
Document title: Groundwater Modelling Analysis
Revision: 3~~1~~
Date: 5 February 2020
Client name: WWLA
Project manager: Jon Williamson
Author(s): Jacob Scherberg, Jon Williamson
File name: G:\Shared drives\Projects\Aupouri Aquifer Water User Group\WWLA0184_Aupouri Aquifer Consents\Deliverables\Aupouri Aquifer Groundwater Model Development Report_2020.docx

Williamson Water Advisory

PO Box 314,
Kumeu 0841,
Auckland
T +64 21 654422

Document history and status

Rev	Date	Description	By	Review	Approved
1	5 March 2019	Internal review	Jacob Scherberg	Louise Soltau	Jon Williamson
2	21 March 2019	Final Review			Jon Williamson
3	5 February 2020	Internal review	Jacob Scherberg		Jon Williamson

Distribution of copies

Rev	Date issued	Issued to	Comments
2	21 March 2019	Public	
3	5 February 2020	Public	Updated following release of LIDAR ground elevation survey data by NRC.

Contents

Figures

Executive Summary

Williamson Water & Land Advisory (WWLA) has undertaken the development of a numerical groundwater model for the Aupouri Aquifer, a shellbed aquifer located on the Aupouri Peninsula of Northland, New Zealand. The purpose of developing the Aupouri Aquifer Groundwater Model (AAGWM) was for evaluating the sustainability of proposed groundwater allocations. To facilitate this, the model compiles all existing information relating to hydrogeological conditions and water use on the Aupouri Peninsula.

The model was developed using the MODFLOW Unstructured Grid (MODFLOW-USG) developed by the United States Geological Survey (USGS) within the GMS10.2 modelling platform.

A conceptual model framework was developed based on a review of 198 bore logs within the model area. Bore logs were interpreted to characterise materials within a basic stratigraphic framework. Four primary layers were identified with their base elevations interpolated between the bore locations. The primary geologic layers used in the model are interbedded dune sand, weathered sand, peat and clay as an upper layer, followed by an upper shellbed, a layer of compact sand, and a lower shellbed. The shells beds comprise the primary aquifer in the model. The lower model boundary was determined by interpolating the elevation where basement rock was encountered as noted in bore logs.

The upper layer of the model was sub-divided into three layers to account for surface conditions and heterogeneity within the material. The upper model layers were classified into coastal sand, weathered sand, and clay/peat, based on soil types.

Climate data and water use data were evaluated to develop a time series data set for groundwater recharge and groundwater pumping.

Time series observations of groundwater levels were available from 56 bores. This data was the basis for model calibration. A steady state model was first calibrated to determine an initial estimate of parameter values and initial conditions for the transient model.

The model was calibrated in both steady state and transient modes, with the most weight given to transient calibration as this reflects long term temporal change. The mean of the RMSE for all gauges was 1.31 m, which is 5.0% of the observed range in groundwater head (26.5 m), while the RMSE for all groundwater level measurements used for model calibration was 1.48 m, or 5.6 % of the range of observations. A simulated RMSE of less than 10% of the measured range is considered a good calibration so both analysis criteria meet this standard. Temporal variability in groundwater levels was well simulated throughout the model while there was, in some cases, a discrepancy between simulated and observed groundwater elevation.

This report documents the methodology applied in the development of the AAGWM and presents the factual results of this modelling study.

1. Introduction

Williamson Water & Land Advisory (WWLA) has undertaken the development of a numerical groundwater model for the Aupouri Aquifer, a shellbed aquifer located on the Aupouri Peninsula of Northland, New Zealand. The purpose of developing the Aupouri Aquifer Groundwater Model (AAGWM) was for evaluating the sustainability of proposed groundwater allocations. To facilitate this, the model compiles all existing information relating to hydrogeological conditions and water use on the Aupouri Peninsula.

The Aupouri aquifer is managed by the Northland Regional Council (NRC) and is divided into ten allocation zones for management purposes (**Figure 1**), with the total amount of groundwater available for pumping within each management zone based on 15% of estimated total recharge for the given zone. The process of developing the AAGWM has entailed an assessment of both natural conditions and management practices related to the following aspects of the model area:

- Geologic and hydrogeologic conditions;
- Climate records over the past 60 years;
- Aquifer recharge based on rainfall and ground cover;
- Current and historic groundwater use;
- Surface water, including lakes, streams, and agricultural drains; and
- Coastal conditions with regard to ongoing or potential saline intrusion into the aquifer.

Consideration of these aspects of physical conditions within the Aupouri Peninsula were the basis for developing a conceptual framework that was used as the basis for the numerical model. A transient simulation of groundwater levels was calibrated to data from monitoring piezometers located within the model area. The hydrological parameters were assigned on the basis of known characteristics from test pumping of the predominant materials within the model domain.

The calibrated model was used to quantify the water balance for the entire Aupouri aquifer, making the model a tool that can be used to evaluate changes in the water balance that may result from management proposals or variability in climate.

Model development has progressed over time as new information has become available and in response to feedback and questions received as part of the Independent Peer Review process that was commissioned by NRC. **Table 1** provides a summary of the major changes that have been implemented since the publication of the original model.

Figure 1. Project locality map. (See A3 attachment at rear).

Table 1. Development history of AAGWM and preceding Aupouri Aquifer models developed by WWLA.

Date	Document	Comments
8/03/2018	Motutangi-Waiharara Groundwater Model Report	The Motutangi-Waiharara Water User Group (MWWUG) groundwater model, a predecessor of the AAGWM, was developed to support the MWWUG groundwater take applications (17).
3/08/2018	Waiharara-Paparore Groundwater Model	The Waiharara-Paparore groundwater model, another predecessor of the AAGWM, was developed to support the Valic, Tiri, and Wataview Orchards groundwater take applications.
29/11/2018	Te Raite Station Groundwater Investigation	The initial version of the AAGWM was completed to support the groundwater take application for Te Raite Station. Calibration efforts were focused on the area from Paparore to Ngataki.
10/04/2019	AAGWM AEE Addendum	A document prepared to provide supplemental information based on model results in response to S92 comments/requests from NRC and independent reviewers in regard to the Te Raite Station application. Specific matters that were addressed included: • Annual versus daily pumping volumes in the model. • Analysis of cumulative drawdown effects for all groundwater pumping relative to naturalised conditions. • Explanation of potential saline intrusion analysis methods. This document was updated on 14/8/2019 to include the proposed groundwater take for Mervyn Evans (App.040979.01.01).
14/05/2019	Aupouri Aquifer Groundwater Development Report	The AAGWM was revised and updated to include proposed groundwater takes for Sweetwater Farms. Monitoring wells on and around the Sweetwater Farms properties were included in model calibration.
16/05/2019	AAGWM Cumulative Lateral Migration Assessment	Assessment of maximum potential saline intrusion along the coastal margins on the AAGWM model area under naturalised conditions and with proposed groundwater extraction. Updated maps are provided showing areas potentially subject to saline intrusion. The model boundary was revised to include inlets that were previously cut out of the model because this resulted in an artificial no-flow boundary condition where, in practice, groundwater would be able to flow beneath the inlet. Instead a constant head boundary condition with 0 mAMSL pressure was incorporated into Layer 1 in these areas. The model grid was revised accordingly and model results improved.
24/09/2019	NRC Notification Maps	Maps showing maximum predicted drawdown at registered bore in the model area for the purpose of notifying potentially affected parties of the pending groundwater take applications.
5/02/2020	Updated AAGWM Development and Calibration	AAGWM updated based on LIDAR Elevation data provided by NRC and associated changes to model structure based on the revised elevation data. The improved data resolution allowed for an improvement in model calibration.
5/02/2020	Updated Assessment of Environmental Effects for Aupouri Aquifer Groundwater Take Applications	Updated analysis of relative and cumulative drawdown, potential saline intrusion, and land settlement based on the updated AAGWM.

This report is a comprehensive documentation of the methodology applied in the development of the AAGWM and presents the factual results of this modelling study. Separate assessment of environmental effect (AEE) reports have been prepared by WWLA for 23 of the groundwater take applicants. This report and the accompanying AEE report supersede previous information derived from numerical model analysis. Other components of the individual AEE's that have been submitted remain unchanged for the documents lodged with NRC.

1.1 Report Structure

The structure of this technical report is as follows:

- **Section 2** provides an overview of the conceptualisation of the groundwater flow model.
- **Section 3** details the model construction and configuration.
- **Section 4** details the calibration of the steady-state and transient models.
- **Section 5** provides a summary of the key findings and conclusions of this project.

2. Model Conceptualisation

This section describes the conceptualisation of regional hydrogeological conditions and the methods applied in representing these conditions in the numerical groundwater flow model.

2.1 Topography

The original topographic model or Digital Elevation Model (DEM) used in this project was based on the LINZ 8-m resolution dataset. However, as alluded to in **Table 1,** in December 2019 a LIDAR survey commissioned by NRC was made available. This enabled an update to the DEM at a much greater level of detail of 1-m resolution. The new LIDAR DEM was used to define the ground surface elevation and confirm unsurveyed bore collar elevations over the model area.

2.2 Soils

The western to central part of the project area is predominately comprised of sandy brown soils. Along both coastal strips there are coastal dunes, which are windblown and unconsolidated, with little to no soil development and excessive drainage hydraulic properties.

The eastern area is mixed with a variety of peat, sand and pockets of clay soils. The prevalent soils in the eastern areas are loamy peat and peaty sand. The loamy peat soils are organic, characterised by high water available capacity and low bulk density. The peat in these soils is moderately decomposed.

The peaty sand soils are pan podzols, which have cemented pans within the B horizon and have naturally low fertility and low permeability, limiting root depth.

It is interesting to note that most boreholes display units of peat and iron pan at multiple depths, suggesting the sand dune sequences have shifted in location and hence are highly dynamic through geological time.

Long-time local farmers and orchard developers provided the following anecdotal information on iron pans:

- "The iron pans vary in both thickness and number of layers" (pers. com. Stanisich, Broadhurst, Hayward).
- "There are multiple layers of pan at varying depths and our pan breaking for planting rows only seems to create vertical drainage at the top" (pers com. McClarnon).
- "Monitoring of bores screened in different zones during test pumping often show no effect at shallower levels to the pumping bore, indicating some separation of zones" (pers. com. Stanisich, Hayward).
- "From bore logs, iron pans are often recorded as consolidated brown sands. However, these may not be the only confining layers. Consolidated mica sands and silts are also good barriers" (pers. com. Stanisich).

2.3 Geology

The geology of the Aupouri Peninsula consists of Pleistocene and Holocene unconsolidated sedimentary materials deposited in beach and dune (abandoned shorelines and marine terraces) and associated alluvial, intertidal estuarine, shallow marine, lakebed and wetland environments.

The geologic units in the model domain were identified through the available bore logs sourced from NRC. The sediments near the surface typically comprise fine-grained sands, interspersed with sporadic iron pan, peat, lignite, silt, gravel and shellbeds.

With distance inland from the coast, the sand deposits become progressively older and have a higher degree of compaction and weathering compared to the younger foredune sands located at the coast.

With increasing depth, the occurrence of shellbed layers increases. The shellbeds comprise layers that typically range in composition from 30-90% medium to coarse shell and 10-70% fine sand. The shellbed aquifer typically resides from approximately 70 to 120 mBGL and is the most prolific water yielding aquifer in the region, hence the target for irrigation bores.

Underlying the shellbed aquifer are basement rocks of the Mount Camel Terrain, which typically comprise hard grey to dark green / black igneous rocks described in Isaac (1996) as intercalated basalt and basaltic andesite lava, pillow lava, rhyolitic tuff, tuff-breccia, with sedimentary deposits of conglomerate, sandstone and mudstone also present.

Drilling data from bores in the Aupouri aquifer indicates that the sedimentary sequence can be broadly classified into two lithological units. The upper bulk layer comprises the fine-grained sands, interspersed with iron pan, peat, lignite, and silt. The lower layer comprises mostly shellbeds, although recent drilling has identified the existence of two discrete shell units separated by a thin fine sand or silt layer, hence the lower layer is sub-divided into three distinct layers. The lithological unit classification developed for this study is exemplified in **Figure 2A** and **Figure 2B** using three reliable bore logs, and is described as follows:

- ***Layer 1 – Sand / Silt.*** A sequence of predominately unconsolidated fine sand intersperses with discontinuous layers of alternating iron pan, silt and peat. The layer varies in thickness from approximately 45 m to 110 m with the thickest regions located around the model area peak elevations.
- ***Layer 2 – Upper Shellbed.*** A sequence of shellbeds comprising medium to coarse shell with some fine sand in the matrix. The proportion of shell typically varies from 30% to 90%. The layer is typically encountered at a depth of 60 - 110 mBGL and varies in thickness from typically 5 m - 15 m.
- ***Layer 3 – Sand.*** A thin layer of finer sediment separating the upper and lower shellbed.
- ***Layer 4 – Lower Shellbed.*** A sequence of shellbeds typically comprising a higher proportion of shell with coarser grain size than the upper shellbed. In some locales, the shell is more consolidated and described by drillers as shell rock. Drillers also report circulation losses when drilling this formation. The layer is typically encountered at depths of 80 - 145 mBGL and varies in thickness from typically 5 m - 30 m.

Honey Tree Farm Bore
(Drilled on 20 June 2016)

From (mBGL)	To (mBGL)	Lithology
0	1	Brown pan
1	4	Brown sands
4	5	White/green sands
5	8	Brown sands
8	22	Grey/brown Sands
22	37.6	Very fine green/grey sands
37.6	38.4	Brown silt
38.4	40.1	Grey silt
40.1	42.2	Fine brown/grey sands
42.2	47	Green/grey sandy silts
47	58	Green sandy silt-some shell
58	58.9	Cemented black sand
58.9	60	Shellbed 40% shell
60	65	Shellbed 70% shell
65	68	Coarse shells, gravels
68	72.6	80% shell/coarse gravel 30mm
72.6	72.8	Silty sand
72.8	82	Fine sands, some shell
82	83	10% shell/ sand
83	110	Consolidated shell - soft shell - rock
110.3	110.7	Grey soft rock
110.7	111.6	Harder black rock

Model layers: Layer 1 - Sand/Silt; Layer 2 - Upper Shellbed; Layer 3 - Sand; Layer 4 - Lower Shellbed

Mapua Orchard Bore
(Drilled on 19 April 2017)

From (mBGL)	To (mBGL)	Lithology
0	6	Brown dune sands
6	12	Green/grey sands
12	15	Black sandy peat/silts
15	24	Fine grey sands
24	25	Brown organic silts
25	28	Brown fine sand, silica
28	29	Peat/timber
29	40	Silica sands/brown sands
40	44	Fine grey sands/silica
44	47	Brown sands/organic silts
47	48.5	Grey sandy silt
48.5	60	Clean fine grey sands, Mica
60	62	Grey sands, flecks of organics
62	82	Dark grey sands, some black sand
82	83.2	Fine black/grey sand
83.2	86	30% Medium shell
86	87	50% Medium shell
87	91	60% Medium shell
91	94	Fine sand, traces of shell
94	97	60% Medium/ coarse shell, a few lenses of silt. Balance sand
97	98	50% M/c blk shell
88	99	60% M/c blk shell
99	101	90% Medium/coarse black shell
101	102	Fine grey sand
102	103	90% Coarse blk shell
103	104	70% Coarse blk shell
104	105	50% Coarse blk shell
105	106	25% Coarse blk shell
106	107	40% Coarse blk shell
107	108	30% Coarse blk shell
108	110	Fine grey sand, shell fragments
110	111.4	30% Coarse shell
111.4	112	Dark grey rock

Model layers: Layer 1 - Sand/Silt; Layer 2 - Upper Shellbed; Layer 3 - Sand; Layer 4 - Lower Shellbed

Largus Orchard Bore
(Drilled on 12 April 2017)

From (mBGL)	To (mBGL)	Lithology
0	1	Golden dune sand
1	4.5	Peat and timber
4.5	18	Brown/green fine sands
18	42.7	Grey/white sands
42.87	45.5	Firm grey sandy silts
45.5	47	Brown peaty silts
47	53	Brown/grey fine sands
53	63	Green/grey fine sands, some thin bands fine gravel
63	67.5	Sandy silt, flecks of shell
67.5	68.5	Cleaner silt, shell
68.5	73	Grey silt
73	74.1	Cleaner sand, shell
74.1	76	60% Coarse shell
76	77	20% Coarse shell
77	78	50% Coarse shell
78	80	20% Coarse shell
80	83	70% Coarse shell
83	84	50% Coarse/med shell
84	86	50% Medium shell
86	88	30% Medium shell
88	89	50% Medium shell
89	91	30% Medium shell
91	93.6	50% Coarse/med shell
93.6	93.8	Light green silt
93.8	105	Firm, clean, grey/white shell rock
105	106	Softer mushy shell rock
106	107	Clean firm shell rock
107	110.9	Softer mushy shell rock

Model layers: Layer 1 - Sand/Silt; Layer 2 - Upper Shellbed; Layer 3 - Sand; Layer 4 - Lower Shellbed

Figure 2A. Lithological unit classification from example borelogs.

Valic-1
(Drilled on 16 August 2006)

From (mBGL)	To (mBGL)	Lithology
0	1	Fine sand-brown
1	2	Fine sand-dark brown
2	4	Fine sand-light brown/grey
4	6	Fine sand-light orange/brown
6	13	Fine sand-light orange/brown. Trace organics
13	15.5	Fibrous peat with wood/roots. Black
15.5	18	Fine sand-dark brown/grey. Siliceous. Trace mica
18	20	As above-becoming greyish brown
20	26	Fine sand-dark brown/grey. Siliceous. Trace mica
26	29	Amorphous peat, dark brown/black
29	33	Fine sand, dark brown/brownish grey
33	45	Fine sand, dark brown/brownish grey. Minor medium to coarse sand (quartz/silica). Trace mica
45	52	Fine to medium sand-grey
52	56	Medium sand, greyish brown. Minor coarse sand quartz/silica and mica
56	62	Fine sand-orange brown
62	67	Fine sand as above becoming grey
67	68	Fine-med brown
68	75	Fine sand , greenish grey, glauconitic, siliceous, minor mica
75	83	Fine sand-greenish grey with minor mica; glauconitic, siliceous
83	85	Fine sand as above. Trace fine shell
85	86	As above, coarser shell
86	88	Fine grey sand. Coarse shell up to 40%
86	90	Fine sand. 10% Coarse shell
90	93	Silty fine sand with marine mud. Trace fine to coarse shell
93	98	Silty fine sand with marine mud. Coarse shell 10-40% increasing with depth
98	100	Coarse granular shell (65%) with fine grey
100	108	Fine sand, grey. 10% shell
108	117	Fine sand, grey, trace shell

Model layers
Layer 1 - Sand/Silt
Layer 2 - Upper Shellbed
Layer 3 - Sand
Layer 4 - Lower Shellbed

George Ujdar Bore
(Drilled on 06 April 2006)

From (mBGL)	To (mBGL)	Lithology
0	5	Topsoil/brown-grey sand
5	48	Brown/grey sands
48	55	Grey sand
55	74	Brown Sand
74	87	Compacted grey sand
87	92	Brown sand with peate and shell
92	97	Coarse shell
97	101	Fine shell with fine sand
101	104	Coarse shell
104	105	Basement rock

Model layers
Layer 1 - Sand/Silt
Layer 2 - Upper Shellbed
Layer 3-Sand
Layer 4-Lower Shellbed

Sweetwater Monitoring Well 1
(Drilled on 10 October 2007)

From (mBGL)	To (mBGL)	Lithology
0	1	Golden dune sand
1	6	Peat and timber
6	25	Fine brown sand/silt, well sorted
25	27	Peat
27	30	Sandy grey silt, trace shell (fine)
30	36	Peat, black and fibous. Sand content increasing with depth
36	40	Well sorted fine sand, increasingly silty with depth
40	46	Clayey sand, fine, well sorted
46	48	Fine shell
48	51	Peat
51	74	Grey sand, minor silt, clay and fine to medium shell
74	86	Shell bed with minor sand, silt, and fine to medium gravels. Shell fraction 70-90%
86	89	Sandy shell with fine medium grey sand
89	96	Shell bed with fine grey sand, silt. Shell fraction 30-60%
96	98	Sandstone (hard, grey-basement rock)

Model layers
Layer 1 - Sand/Silt
Layer 2 - Upper Shellbed
Layer 3-Sand
Layer 4 - Lower Shellbed

Figure 2B. Lithological unit classification from example borelogs.

2.4 Aquifer Hydraulic Parameters

Groundwater is found throughout the unconsolidated sedimentary materials that occur within the model area, although these materials vary in their ability to store and transmit water, primarily due to grain size, cementation, weathering and compaction.

Test pumping and numerical modelling exercises for irrigation take resource consent applications have been undertaken over the years and summarised in the reports of HydroGeo Solutions (2000), SKM (2007a), SKM (2010), Lincoln Agritech (2015) and most recently by Williamson Water Advisory in 2017 (WWA, 2017). Data from these reports has been reproduced in tables provided **Appendix A**, and is summarised below in **Table 2** where it is presented in the context of our conceptual model as described in the previous section of this report.

Table 2. Summary of previously measured and modelled hydraulic properties for WWLA layer conceptualisation.

Unit	K_x (m/s)			S (-)		
	Min	Max	Arithmetic Mean	Min	Max	Arithmetic Mean
Layer 1 - Sand / silt	$1.0x10^{-5}$	$1.1x10^{-4}$	$8.4x10^{-4}$	Not available		
Layer 2 – Upper shellbed	$2.1x10^{-4}$	$7.3x10^{-4}$	$3.65x10^{-4}$	$2x10^{-2}$	$4x10^{-4}$	$1x10^{-2}$
Layer 3 – Compact sand	$6.9x10^{-5}$	$6.9x10^{-5}$	$6.9x10^{-5}$	$5x10^{-4}$	$5x10^{-4}$	$5x10^{-4}$
Layer 4 – Lower shellbed	$1.3x10^{-4}$	$7.3x10^{-4}$	$4.4x10^{-4}$	$3x10^{-4}$	$4.4x10^{-3}$	$1.6x10^{-3}$

2.4.1 Perched Aquifers and Progressive Confinement

There is anecdotal evidence of localised perched water within the wetlands and lakes in the area. For example, Lake Waiparera, located near the centre of the study area has an average lake stage of 33.8 mAMSL, while the groundwater level measured in an adjacent bore is around 7 mAMSL.

Before the intervention of man, lake and wetland complexes that formed in dune swales were self-accentuating over time. Fine sediment washed into swales with stormwater runoff, and bed permeability progressively decreased due to clogging, which led to widening and deepening of the wetland or lake. As this progressed, acid conditions in the wetland environment led to dissolution of metals and as the sediment substrate conditions shifted from aerobic to anaerobic (or reducing conditions) and pH became more neutral, subsequent precipitation of the dissolved metals occurred as metal hydroxides, particularly iron hydroxide. Iron hydroxide is the primary constituent of iron humus pan or iron pan, which is the main factor (along with peat and silt deposits) in restricting vertical drainage in the Aupouri aquifer.

The aquifer system is unconfined at the surface but behaves in a manner that suggests a progressive degree of confinement with depth (leaky confinement). There is no well-defined regionally extensive confining layer but there are numerous low-permeability layers (e.g. iron pan, brown (organic) sand, silt, peat) that vary in depth and thickness, which over multiple occurrences collectively provide a degree of confinement that lends to the development of vertical pressure gradients, as discussed in **Section 2.7**.

Data collected from shallow and deep monitoring bores shows strong evidence for confinement throughout the model area. The groundwater elevations measured in shallow monitoring bores are substantially higher than the deeper monitoring bores at Sweetwater Farms in the southern portion of the model, Valic Orchards in the middle, and at the Browne and Waterfront monitoring locations in the north portion of the model area. It is likely that this is due to multiple low permeability paleosols (buried iron pans), deeply buried by successive accumulations of sand (Hicks, et. al., 2001).

2.5 Recharge

The proportion of rainfall that infiltrates the soils and ultimately recharges the groundwater system is relatively large, due to the high infiltration capacity of the sandy soils.

The model used in the Aupouri Aquifer Review by Lincoln Agritech (2015) suggested an annual recharge rate of 540 mm or 43% of annual rainfall for the dune sand beneath Aupouri Forest. In other groundwater studies for the region, the percentage of rainfall recharging the dune sands ranged from 10.4% to 43.7%, while for the floodplains the recharge range was 4.2% to 12.0% of annual rainfall (HydroGeo Solutions, 2000; SKM, 2007a; SKM, 2007b).

Climate data obtained from VCSN and select gauging stations within the model area was processed through the Soil Moisture Water Balance Model (SMWBM) to generate the groundwater recharge data set to be used for model input. For the purpose of assessing recharge, the Fundamental Soil Layer (FSL) soil classifications were used to divide the model area into four primary recharge zones based on permeability (**Figure 3**):

- coastal sand;
- weathered sand;
- plains; and
- peat/wetlands.

Variation in rainfall and potential evapotranspiration (PET) across the model area was accounted for by defining four regions along the north-south axis of the model and assigning climate data from an appropriate reference location for each region. The regions, included in **Figure 3**, were referred to as North, Motutangi, Waiharara-Paparore, and South. The recharge zones were then used to determine parameter inputs for SMWBM and generate daily recharge estimates based on the distribution of rainfall across the model area as defined by the climate regions described above. Further details on the process of generating the groundwater recharge data set for use in the model are provided in **Appendix B**.

This assessment resulted in 43% of mean annual rainfall applied as recharge in the coastal sand zone, 38% for the weathered sand zones, 26% for the plains in the southern portion of the model and 10% for the peat/wetlands zones. The work of WWA (2017) has been adopted in this study and is summarised in **Table 3**.

To place these recharge figures in context over the Aupouri Aquifer model domain, in summary:

- mean annual rainfall is approximately 687 billion litres per annum;
- recharge to the aquifer is approximately 236 billion litres per annum;
- the total level of current and proposed allocation is approximately 18 billion litres per annum, which represents:
    - 2.6% of mean annual rainfall; or
    - 7.6% of recharge.

Figure 3. Recharge zones. (See A3 attachment at rear).

Table 3. The average annual water mass balance for each recharge zone from the SMWBM.

Recharge Zone	Groundwater Recharge	Evapo-transpiration	Runoff	Description
Coastal sand zone	43%	48%	9%	Loose sand, high infiltration capacity, low surface runoff
Weathered sand zone	38%	49%	13%	Relatively more compacted sand, high infiltration capacity, reduced surface runoff

Plains zone	26%	54%	20%	Moderate infiltration capacity, medium soil moisture storage, moderate surface runoff
Wetlands/Estuary zone	10%	60%	29%	High peat content, low infiltration capacity, medium soil moisture storage, high surface runoff

2.6 Drainage

In the lower-lying farmland area, there is a man-made drainage network that typically connects to short fetch streams discharging to the coast. The drains were installed to lower the shallow groundwater table to promote more manageable farming conditions (**Figure 4**).

Figure 4. Drainage map. (See A3 attachment at rear).

2.7 Groundwater Level Data

There are 56 reliable monitoring piezometers located within the model area. These can be grouped into three generalized areas which are identified in **Figure 5** as the northern, central, and southern piezometer groups. Many of the piezometers have a nested configuration where up to four piezometers are located together with screened intervals at different depths to simultaneously monitor groundwater levels across a vertical profile. The majority of monitoring piezometers used for model calibration are maintained by the NRC, however some piezometers are privately managed.

The northern piezometer group includes five multi-level piezometers constructed by the Northland Catchment Commission in the 1980s and two single piezometers that are currently maintained for groundwater monitoring purposes in the Houhora area by the Northland Regional Council, collectively defined as the Hukatere piezometer transect.

Figure 6 shows a cross-section of bore depths and static water levels in multi-level piezometers along the Hukatere transect (not-to-scale). The groundwater gradient shown from each piezometer nest is governed by the hydrogeological position of the piezometer on the landscape, i.e. within the recharge or discharge zone. For piezometers that are close to the groundwater divide (Browne piezometer) the observed vertical downward gradient indicates the occurrence of recharge from the surface to the deep aquifers. The piezometers near the coast at the waterfront showed an upward flow potential, indicating groundwater discharge to the sea.

The nested piezometers Burnage 1, 2 and 3 all consistently show similar groundwater levels. It likely that this is due to leakage within the piezometers at this location, thus, these three piezometers were excluded in the model calibration.

The central group of monitoring piezometers, shown in **Figure 7**, includes NRC monitoring bores at Ogle Drive and Paparore. The latter of these has four nested monitoring piezometers ranging in depth from 18 to 75 mBGL. There are four monitoring locations on the Valic Avocado Orchard. Each location features a monitoring bore drilled into the deep aquifer at a similar depth to the nearby production bore and an additional monitoring bore in the shallow aquifer. Vertical hydraulic gradients between the shallow and deep aquifer at the Valic Avocado Orchard range from 6 to 11 meters. By contrast the monitoring piezometers at Paparore measure a minimal vertical hydraulic gradient between the two aquifers, with a slightly greater head measured at the deeper bores relative to the shallow ones.

The southern group of monitoring piezometers are shown in **Figure 8**. The majority of these bores are managed by Sweetwater Farms, where there are 5 pairs of deep and shallow monitoring bores, as well as several additional bores where only one depth is monitored. There are also NRC operated bores at Lake Heather and several independently operated bores where water level data is available, specifically, at Vinac, Waipapa, and Welch.

A vertical downward gradient of groundwater head is evident at Sweetwater Monitoring Wells #1, #3, #4, and #5, though in the case of #4 it is likely that the shallow piezometer is measuring a perched water table based on the groundwater elevation being higher than what is measured in other shallow monitoring wells located further inland. Sweetwater Monitoring Well #2 is the only case where groundwater level measurements indicate an upward groundwater gradient.

Figure 5. Location of monitoring piezometers. (See A3 attachment at rear).

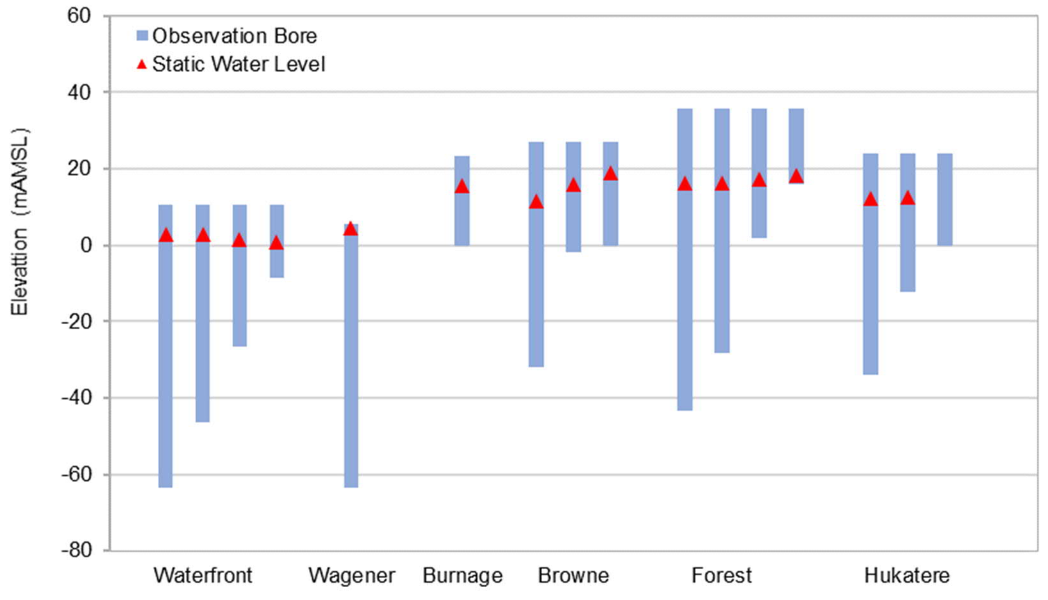

Figure 6. Mean groundwater levels of monitoring piezometers in the northern portion of the model area

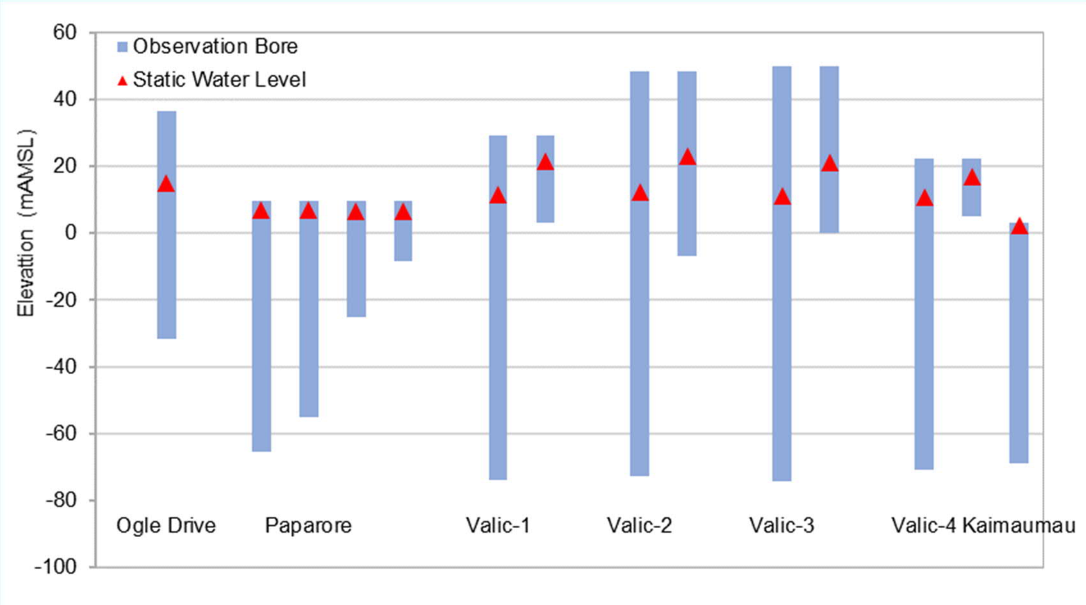

Figure 7. Mean groundwater levels of monitoring piezometers in the central portion of the model area

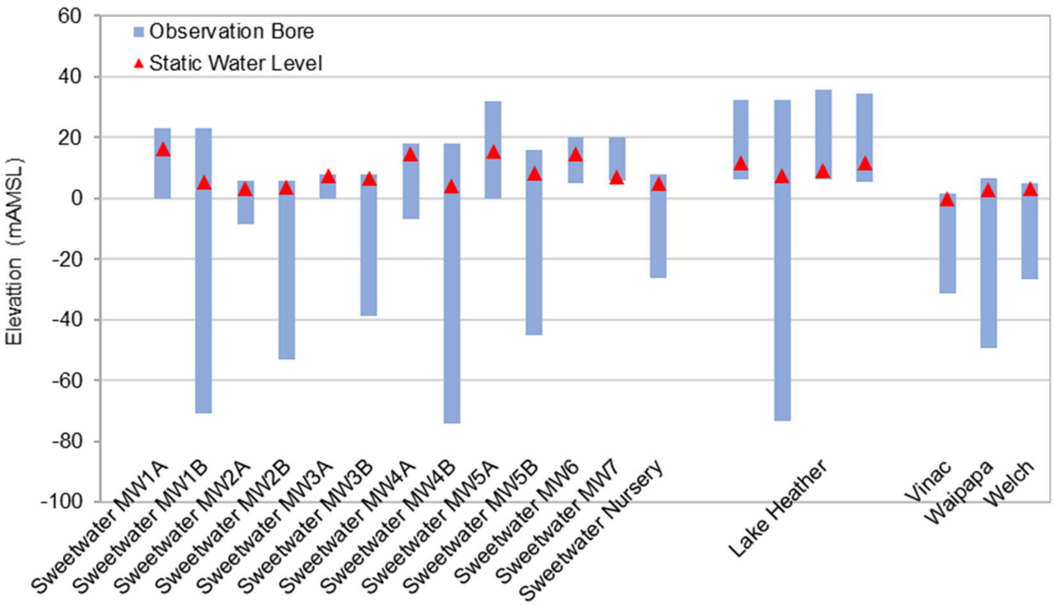

Figure 8. Mean groundwater levels of monitoring piezometers in the southern portion of the model area

2.8 Groundwater Abstraction

Figure 9 shows the location of existing and recently proposed groundwater abstraction consents.

The current level of annual groundwater allocation consented from the Aupouri aquifer is 9.8x10^6 m^3/year (9.8 billion litres per annum) distributed among 88 consents. Some of these consents are exercised through the operation of multiple bores. The currently consented volume stated above includes the Motutangi-Waiharara Water Users Group (MWWUG), although these consents are currently on staged implementation over a seven year period, hence are not currently being exercised to their full consented volumes. Ongoing monitoring of regional groundwater levels and water quality is being undertaken as part of the consent requirements.

In additional to the MWWUG consents, a portion of the consented allocation to Sweetwater Farms, and the full allocation to Far North District Council for the Kaitaia water supply, are not currently being exercised. This equates to over 2.5×10^6 m^3/year (2.5 billion litres per annum).

There are also 28 expired groundwater take consents within the model area, totalling 8.53×10^5 m^3/year (0.85 billion litres per annum) of potential abstraction. These takes were not included in the total amount of currently allocated groundwater, but they were used for developing a historical dataset. **Appendix C** provides consented and proposed groundwater takes corresponding to the locations shown in **Figure 9A** through **Figure** 9**C**.

Figure 9A. Location of existing and proposed groundwater take bores in northern portion of model. (See A3 attachment at rear).

Figure 9B. Location of existing and proposed groundwater take bores in central portion of model. (See A3 attachment at rear).

Figure 9C. Location of existing and proposed groundwater take bores in southern portion of model. (See A3 attachment at rear).

2.8.1 Actual Use Dataset

A historical actual use dataset is required to accurately calibrate a groundwater model and to thereafter use the model to simulate the effects of groundwater extraction on the aquifer and surface water resources.

The SMWBM Irrigation Module was used to develop an estimate of historical actual use. The exercise combined typical irrigation scheduling (Oct - Apr) and the commencement dates that the consents were granted, along with an allowance for orchard development and tree growth rates to maximum water requirement. Details and results of the development of the actual use dataset are provided in **Appendix D**.

A complete dataset of historic groundwater use within the model area was not available, therefore a conservative estimate of groundwater use was generated by assuming that all active consents were available from the beginning of the simulation period with the exception of the two Sweetwater Farms production bores that were known to have initiated operation in 2015 and 2017, respectively and the Valic 1 through 3 production bores where pumping operations are known to have stated in 2007. **Figure 10** shows the total annual volume of simulated actual use as applied in the model.

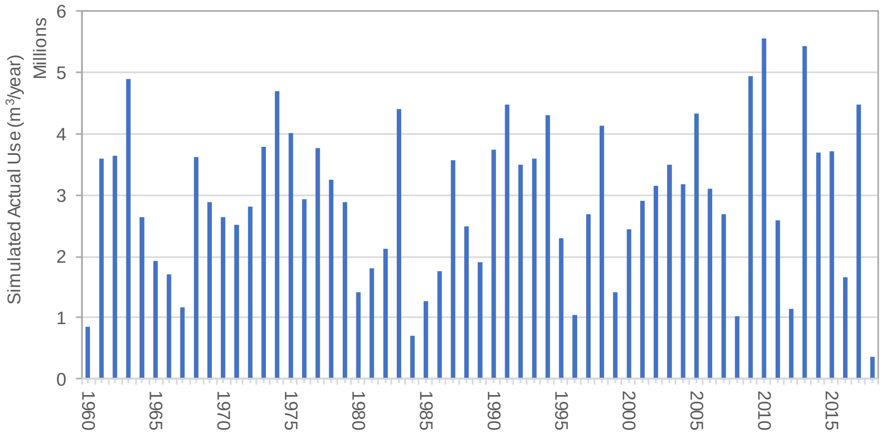

Figure 10. Simulated groundwater extraction (m³/year; partial groundwater use in 2018 due to the end of the model simulation).

3. Model Configuration

The MODFLOW Unstructured Grid (MODFLOW-USG) developed by the United States Geological Survey (USGS) was utilised within the GMS10.2 modelling platform to construct the groundwater flow model in this project. The unstructured discretisation of the model domain provides the capacity of fitting irregular boundaries into the model and increasing the resolution in the areas of maximum interest while decreasing resolution in other areas. This spatially varying discretisation approach reduces model computational time, while maintaining enhanced accuracy of calculation at the points of interest, hence increasing the efficiency in model computation compared to the equivalent regular MODFLOW grid.

3.1 Model Domain

The model was constructed based on six layers, with a total of 92,796 active Voronoi cells (or polygons), and covers an area of 535 km^2. Grid spacing ranges from 40 m at the highest resolution, centred around large groundwater extraction points, to 1,000 m in the northwest portion of the model area where high resolution is unnecessary (**Figure 11**).

Figure 11. Plan view of unstructured model grid discretisation (See A3 attachment at rear).

The boundary conditions included in the model are constant head, general head, drain, and no-flow boundaries.

3.1.1 Constant Head Boundaries

The constant head boundary was assigned an elevation of 0 mAMSL along the eastern and western coastlines in Layer 1 of the model to represent the mean hydraulic head of the ocean at these locations.

3.1.2 General Head Boundaries

A general head boundary (GHB) is typically used to simulate the flow interaction between groundwater and external water sources to the model domain.

There are 22 lakes within the model area that are large enough to occupy the majority of a model cell and were therefore incorporated into the model. It was determined that these lakes occur due to buried hard pans causing localized perching without a direct connection to the regional water table. The conclusion that there is disconnection between surface lakes and regional groundwater is consistent with the findings of other studies such as Lincoln Agritech (2015) and WWA (2017). A GHB was assigned to cells primarily occupied by lakes, to simulate lake water seeping to the underlying groundwater system, with consideration of the impedance provided by the lower-permeability lake bed sediments and/or iron pan. The head stage assigned for the GHB for each lake was determined by extracting the average elevation for each lake based on the model area DEM.

Lake Waiparera, located in the middle the model domain is the largest lake in the model domain. It was observed to have an average lake stage of 31.4 mAMSL while the groundwater level, estimated from the adjacent bore, was around 7 mAMSL, indicating that Lake Waiparera is perched above the regional groundwater system. This is also consistent with the conclusion made in the Aupouri Aquifer Review Report that the main aquifer is situated well below the surface of Lake Waiparera (Lincoln Agritech, 2015).

Similar findings can be demonstrated at Lake Heather where the mean surface elevation of the lake was determined to be 21.0 mAMSL whereas shallow monitoring piezometers located near the lake show groundwater elevations ranging from 9.3 to 11.9 mAMSL.

The cells along the coastline from Layer 2 to 6 were also assigned with GHBs. The head values for all the cells were assigned as 0 mAMSL and the conductance value of each layer decreases with depth. This is to reflect the progressively increasing disconnection of the groundwater with the free water surface of the ocean (i.e. the impedance of flow to the ocean floor increases with depth) and also the resistance of higher-density seawater offshore. It was estimated based on the model calibration that the cells along the west coast boundary had approximately one order of magnitude lower conductance than the cells along the east coast boundary.

3.1.3 No-Flow Boundaries

The AAGWM was designed to encompass the entire Aupouri aquifer therefore no-flow boundaries were assigned to cells located on the northern and southern boundaries of the model domain representing the margin of the aquifer. In the north groundwater is expected to predominantly flow downgradient toward the south and laterally to the coasts while in the south bedrock outcroppings form a boundary to groundwater flow. The base of the model was also assigned a no-flow boundary on the basis that the significantly lower permeability of the basement rocks has negligible bearing on the overall flow budget of the aquifer system above.

3.1.4 Drain Boundaries

Drain boundaries were assigned in the model to simulate the groundwater discharged to the major surface drains, and to simulate the estuary that occurs along the east coast portion of the model area. The drain bed elevations were derived from the LIDAR Digital Elevation Model (DEM), with a nominal depth assignment depending on locality as follows:

- Drains in farmland – DEM minus 2 m;
- Drains in estuary – DEM minus 0.5 m;

The conductance value of the drains was set relatively high to reflect limited impedance to water removal (or drain functionality), to account for the significant water drainage in the farmland area and flow of water over the surface in the wetland.

3.1.5 Well Boundaries

Well points were used to represent the groundwater extraction from within the model. The corresponding model cells were assigned with negative pumping rates to represent the groundwater extraction from the model.

3.2 Simulation Package

3.2.1 Sparse Matrix Solver

The Sparse Matrix Solver (SMS) package was utilised to solve linear and non-linear equations. A maximum head change of 0.01 m between iterations was set as the model convergence criteria. Default values were used for the maximum number of iterations for linear and non-linear equations.

3.2.2 Ghost Node Correction Package

MODFLOW-USG is built on the control volume finite difference formulation, which enables the model cell to be connected to an arbitrary number of adjacent cells (Panday et al., 2013). However, this formulation will be reduced to a lower order of approximation, when the line between two connected nodes does not bisect the shared face at right angles, which will lead to errors in the simulation (Edwards, 1996). To account for this, the ghost node correction package was utilised to improve the simulation results by adding higher order correction terms in the matrix solver. Ghost nodes are implicitly built into the simulation through the interpolation factors. The simulated head is systematically corrected through the ghost nodes to achieve a correct solution.

3.3 Model Layer Configuration

3.3.1 Layer Geology

The model comprises six layers that are used to represent the varying geology located in the area. As indicated in **Section 2.1**, a digital elevation model with 1-m resolution derived from a LIDAR survey commissioned by NRC was used to determine surface elevation over the model area. The thickness and base elevation of underlying layers was defined by an analysis of bore geologic information recorded in borelogs distributed over the model area. The geological units assigned to each layer of the numerical model are shown in **Table 4**.

Table 4. Geological units in the model conceptualisation.

Model Layer	Stratigraphic Layer	Name	Description	Locality
1-3	1	Coastal sand	Loose coastal sand, highly permeable	Western and eastern coastal strips.
	1	Weathered sand	Weathered dune sand, moderately compacted	Inland hilly or rolling country areas.
	1	Wetland/Estuary	Peaty and clayey sediments, low permeability	Low lying region along east coast including Kaimaumau wetland. Only applied for Model layer 1.
	1	Plains	Peaty and clayey sediments with some sand, low-moderate permeability	Inland low-lying plains areas in southern region of model. Only applied for Model layer 1.
4	2	Shellbed	Sand presented with shells, highly permeable	Throughout model, albeit thickness varies.
5	3	Fine sand	Old sand deposits, fine sand, moderately permeable	
6	4	Shellbed	Sand presented with more shells, highly permeable	

Model Layers 1-3 are used to represent a complex stratigraphic unit comprising alternating sands, silt, peat, clay and iron pans in a bulk sense (not discretely). The sub-division of this stratigraphic unit into layers is complex because layering is varied both horizontally and vertically. For modelling purposes, horizontally continuous and vertically discrete layers are required to enable anisotropy to be incorporated in the model calibration process; hence the base of model Layer 1 was defined as an elevation of -2.0 mAMSL, while the base of model Layer 2 was set at 22 m above the base of model Layer 3. Based on the 10 m vertical hydraulic gradient observed in the monitoring data at Valic-2 from the Valic-2 shallow and deep piezometers, it is likely that there is a localised zone of low permeability in the subsurface in this region. This was incorporated into the model as a limited region of low conductivity relative to the surrounding material.

All model layer bases other than model Layer 1 and 2 conform to stratigraphic interpolations as discussed in the following section.

3.3.2 Layer Elevations

The top and bottom elevation for the geological unit contacts were determined through a process of reviewing 198 bore logs at locations within the model area. The majority of the bore logs were obtained by request through the NRC while some additional bore logs were provided directly through the bore owners. Each bore log was reviewed to characterise the primary material types within the context of the conceptual geological configuration incorporated into the model. The bottom elevations for each unit were interpolated using the Kriging geospatial method to generate a digital elevation surface.

The geometry of the interface between the lower shellbed and basement rocks has been recognised through interpolation of the basal contact from the available bore logs in the area.

During interpolation, rules were applied so that geological layers did not overlap, and the surface is stratigraphically continuous.

Figure 12 through **Figure 15** show interpolated elevation contours used for the model layer interfaces and basement elevation (i.e. the model bottom).

Figure 12. Bottom elevation of sand and peat layers (model Layers 1-3 base). (See A3 attachment at rear).

Figure 13. Bottom elevation of upper shellbed (model Layer 4 base). (See A3 attachment at rear).

Figure 14. Bottom elevation of compact sand layers (model Layer 5 base). (See A3 attachment at rear).

Figure 15. Basement rock elevation contours (model Layer 6 base). (See A3 attachment at rear).

Geological cross-sections were developed from selected transects through the kriged surfaces in north-south (N-S) and west-east (E-W) directions to demonstrate the relative thickness of each geological unit. Transects are identified by the section of the model where they are located and are shown in **Figure 16** while the cross-sections themselves are shown in **Figure 17** to **Figure 24**. The constructed model grid based on the interpolated layer elevations is shown in **Figure 25**.

Figure 16. Hydrogeological cross section locations. (See A3 attachment at rear).

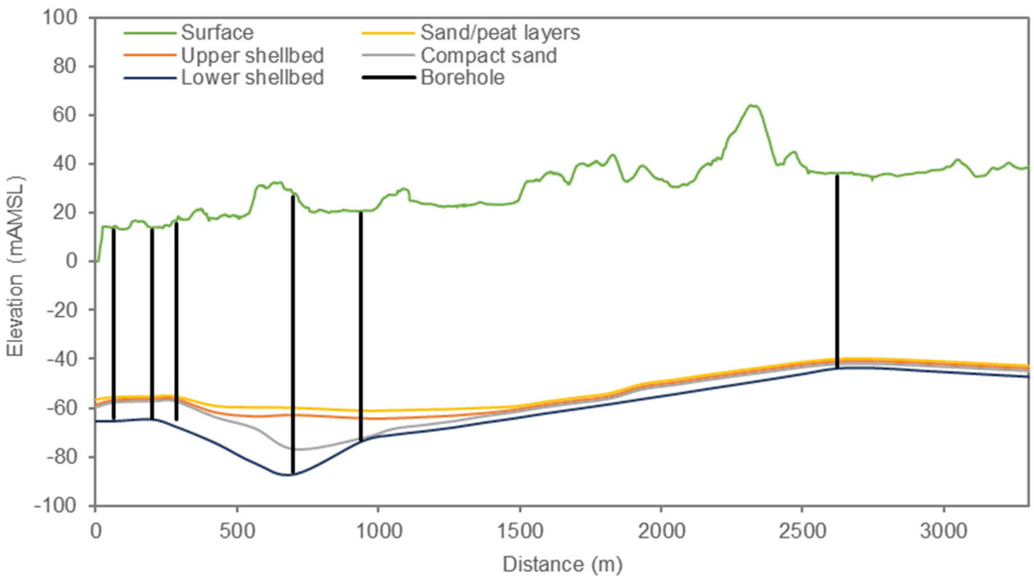

Figure 17. Interpolated cross-section A to A’ showing bore locations (refer to Figure 16 for location).

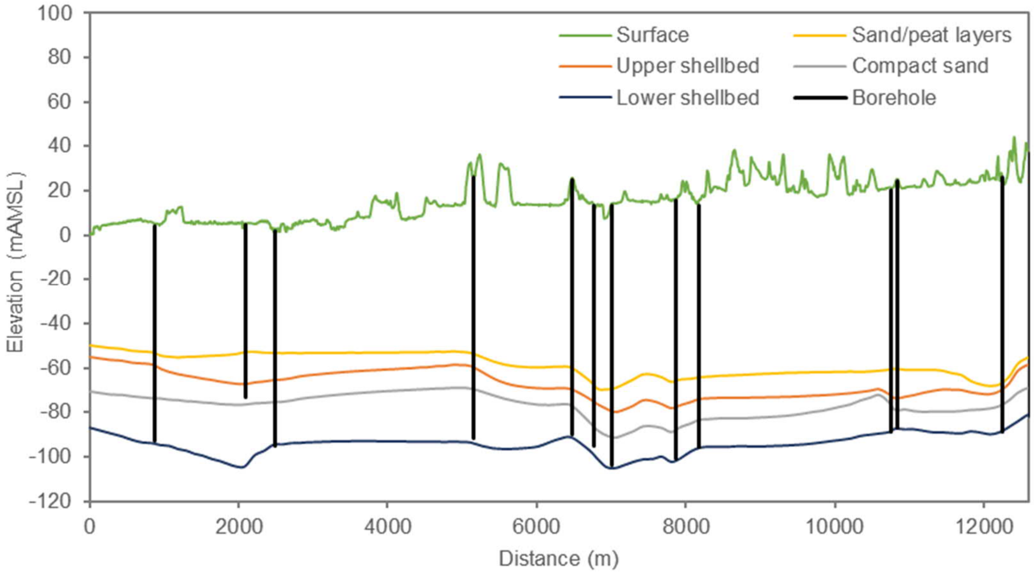

Figure 18. Interpolated cross-section B to B' showing bore locations (refer to Figure 16 for location).

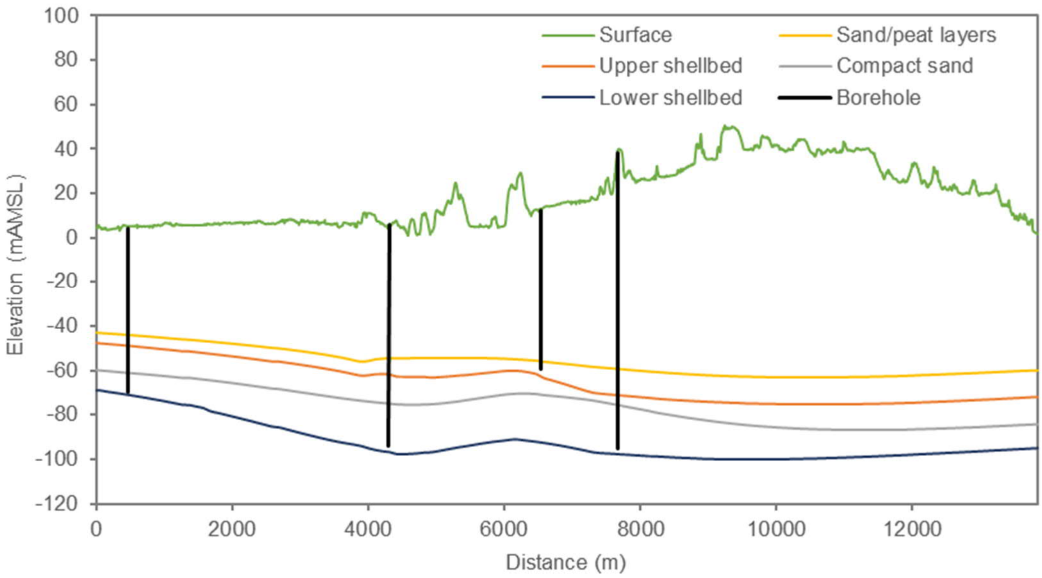

Figure 19. Interpolated cross-section C to C' showing bore locations (refer to Figure 16 for location).

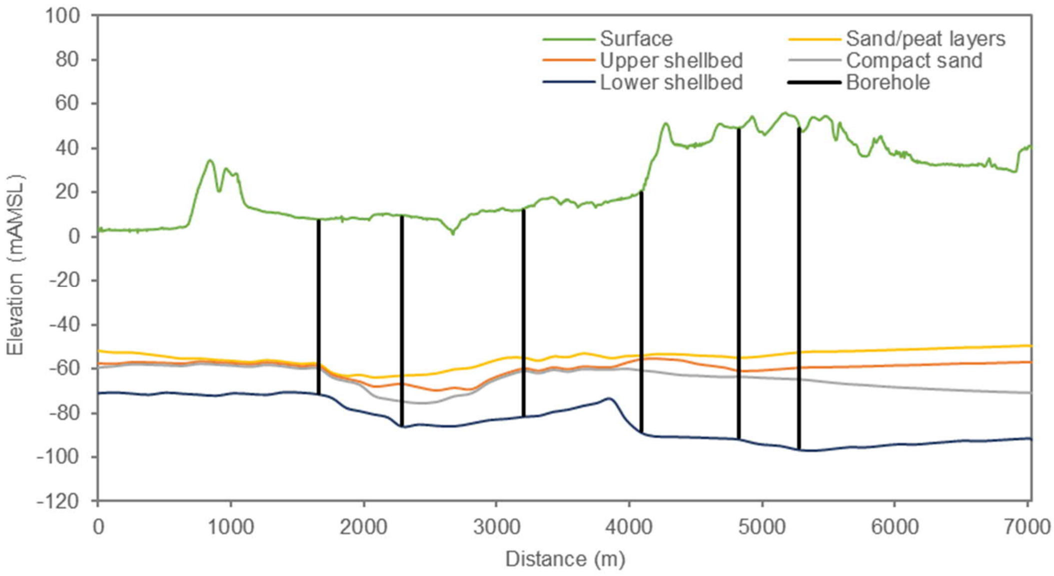

Figure 20. Interpolated cross-section D to D' showing bore locations (refer to Figure 16 for location).

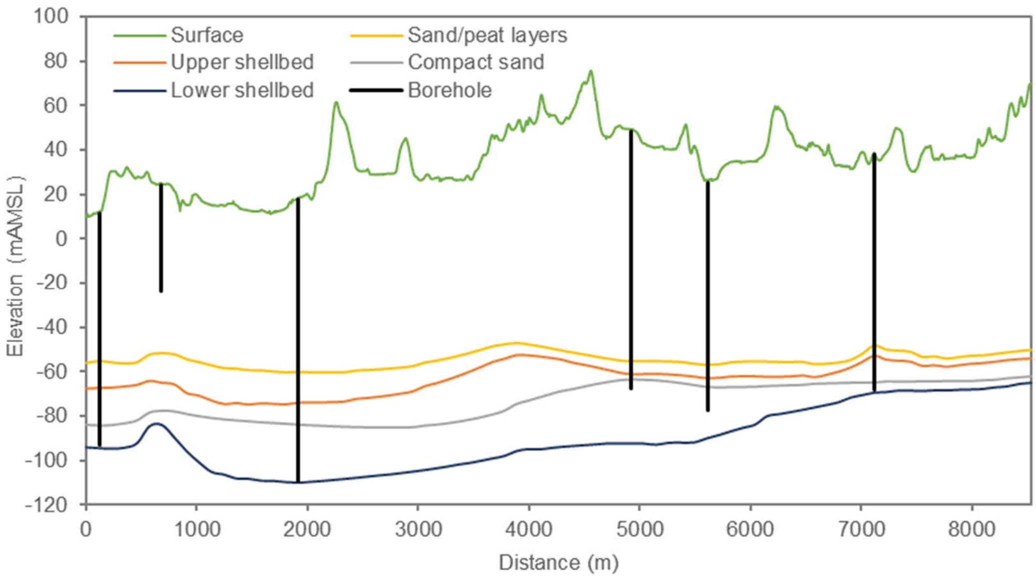

Figure 21. Interpolated cross-section E to E' showing bore locations (refer to Figure 16 for location).

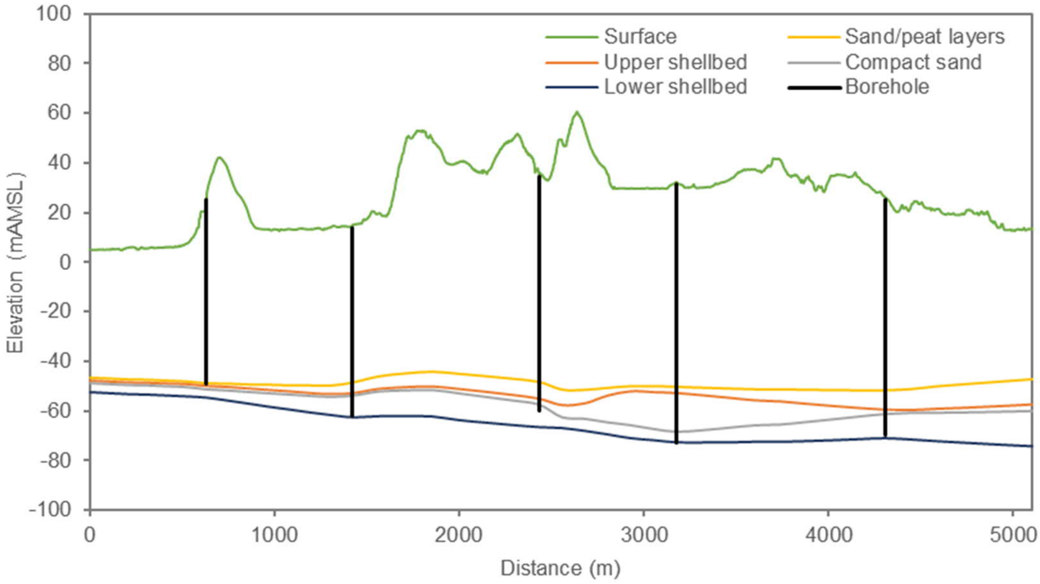

Figure 22. Interpolated cross-section F to F’ showing bore locations (refer to Figure 16 for location).

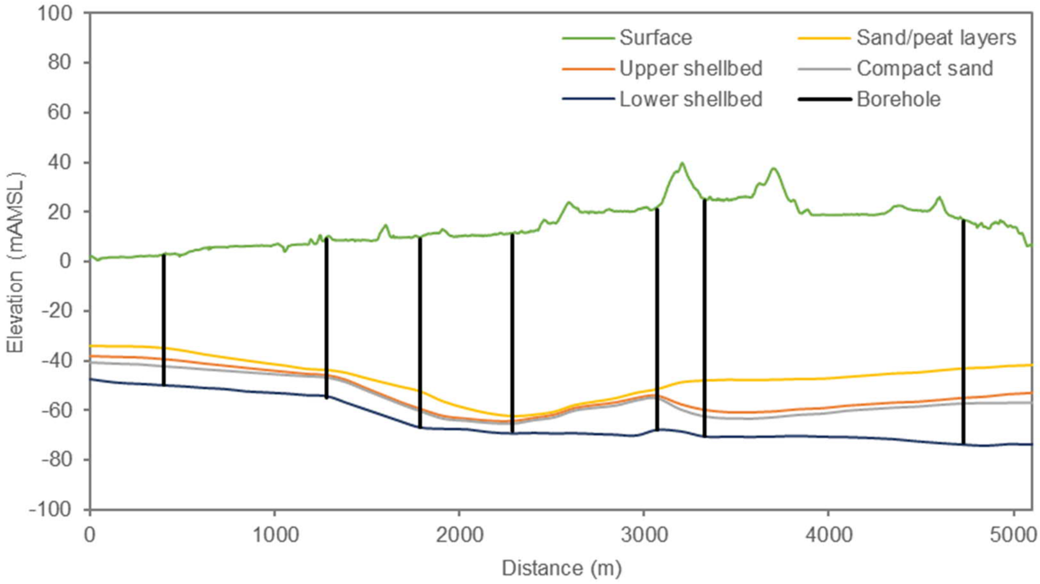

Figure 23. Interpolated cross-section G to G’ showing bore locations (refer to Figure 16 for location).

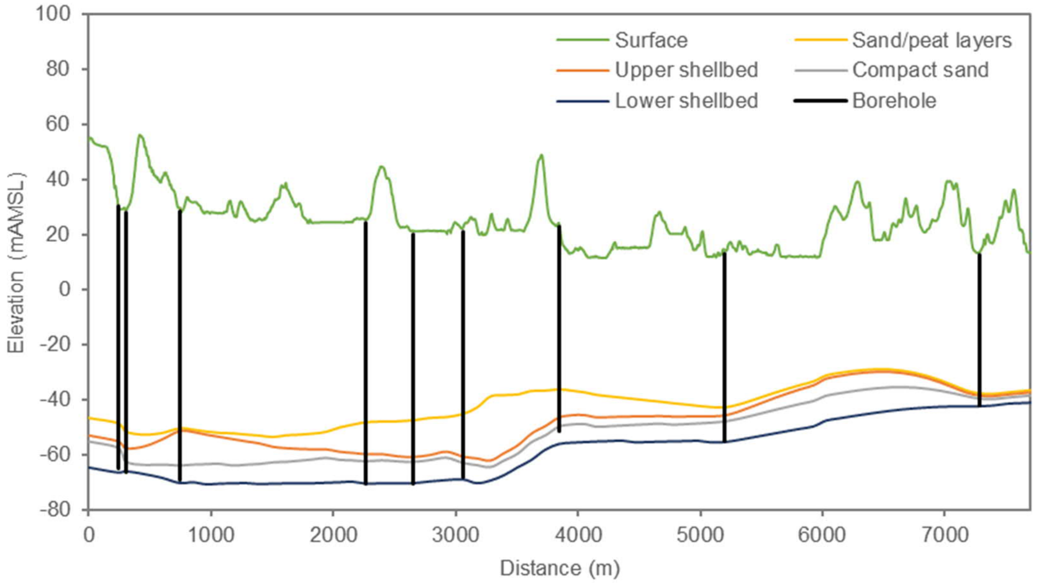

Figure 24. Interpolated cross-section H to H' showing bore locations (refer to Figure 16 for location).

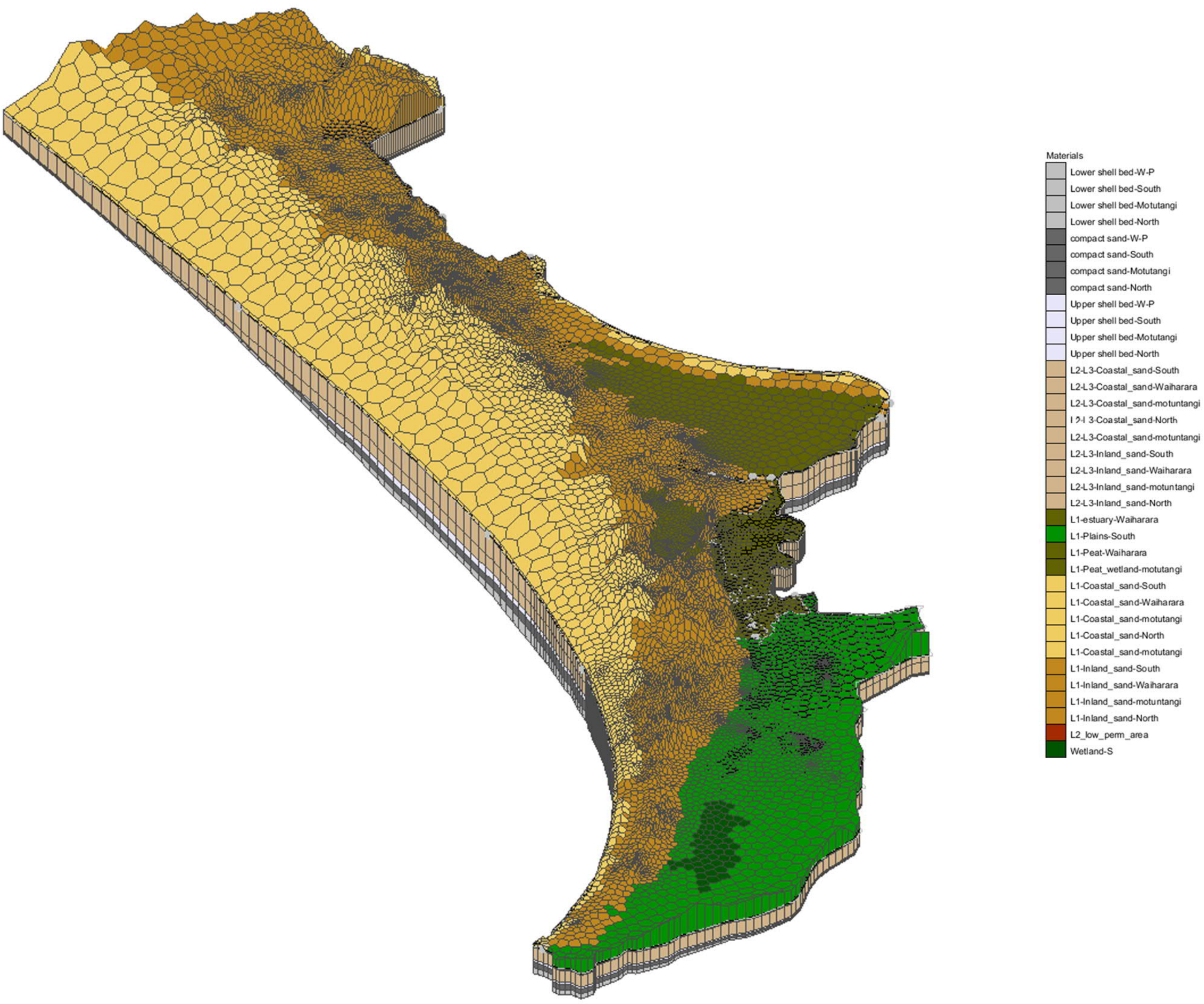

Figure 25. MODFLOW grid with vertical magnification of 25.

4. Model Calibration

The model calibration was conducted by changing the model hydraulic parameters to achieve an acceptable fit to measured groundwater levels, which was undertaken using both automated and manual proceedures. Groundwater recharge was not considered a calibration parameter.

4.1 Observation Points

The piezometers used for calibration of the model are shown in **Figure 5** and the key properties of the piezometers relevant to model calibration are summarised in **Table 5**. The piezometers include nested piezometer configurations comprising adjacent standpipes installed to different depths or aquifer levels and standalone piezometers measuring a single depth. Vertical pressure gradients are evident where there are concurrent measurements from nested piezometers measuring different depths at a single location.

Achieving a simulated vertical pressure gradient requires multiple layers with vertical anisotropy to be incorporated in the model (as discussed in **Section 2.7**). To achieve this, a finer vertical discretisation of the model was required, and this was a key driver for splitting stratigraphic Layer 1 into three model layers as described in **Section 3.3**. The discrete layers enabled vertical anisotropy to be considered in model calibration as a bulk property within each layer while providing flexibility to vary anisotropy vertically to account for the heterogeneous nature of the materials.

Table 5. Key specifications of the observation bores used for model calibration.

Model Region	Site	Piezometer Description	Mean groundwater level (mAMSL)	Standard deviation (m)	Bore depth (m)	Model Layer
Hukatere Transect	Waterfront	NRC shallow monitoring bore	0.94	0.36	19.0	2
		NRC middle monitoring bore	1.47	0.36	37.0	2
		NRC deep monitoring bore	2.81	0.28	57.0	3
		NRC deep monitoring bore	2.78	0.29	74.0	4
	Hukatere	NRC shallow monitoring bore	13.79	1.26	19.0	1
		NRC middle monitoring bore	12.68	1.15	36.0	2
		NRC deep monitoring bore	12.26	1.11	58.0	2
	Forest	NRC shallow monitoring bore	18.51	1.07	16.0	1
		NRC middle monitoring bore	17.53	1.31	36.0	1
		NRC deep monitoring bore	16.26	1.17	64.0	2
		NRC deep monitoring bore	16.25	1.17	79.0	3
	Burnage	NRC shallow monitoring bore	15.61	0.71	17.0	1
	Browne	NRC shallow monitoring bore	18.86	0.93	16.0	1
		NRC shallow monitoring bore	16.00	0.82	29.0	1
		NRC deep monitoring bore	11.72	0.78	59.0	2
	Wagener Golf Club	Deep monitoring bore	4.48	0.28	69.0	4
	Fishing Club at Houhora	Deep monitoring bore	3.65	0.61	78.0	5

Model Region	Site	Piezometer Description	Mean groundwater level (mAMSL)	Standard deviation (m)	Bore depth (m)	Model Layer
Waiharara-Paparore Region	Kaimaumau Deep	NRC	2.44	0.82	72.0	6
	Ogle Drive	NRC Monitoring Bore	14.90	0.32	68.0	2
	Paparore	NRC deep monitoring bore	6.88	0.66	75.0	6
		NRC deep monitoring bore	6.88	0.63	65.0	6
		NRC middle monitoring bore	6.46	0.26	35.0	2
		NRC shallow monitoring bore	6.42	0.27	18.0	2
	Valic-1	Shallow Monitoring Bore	21.74	0.47	17.0	1
		Deep monitoring bore	11.65	0.83	103.0	6
		Production Bore	11.41	0.83	103.0	6
	Valic-2	Shallow Monitoring Bore	22.88	0.77	55.0	1
		Deep monitoring bore	12.24	1.00	121.0	6
		Production Bore	12.06	0.85	121.0	6
	Valic-3	Shallow Monitoring Bore	20.99	0.76	45.0	1
		Deep monitoring bore	11.28	1.94	124.0	6
		Production Bore	11.32	2.23	124.0	6
	Valic-4	Shallow Monitoring Bore	16.75	0.60	13.0	1
		Deep monitoring bore	10.77	0.54	93.0	6
		Production Bore	10.75	0.55	93.0	6
Sweetwater Farms Monitoring Wells	Sweetwater MW1	Shallow Monitoring Bore	16.25	0.48	13.3	1
		Deep monitoring bore	5.22	2.13	94.0	6
	Sweetwater MW2	Shallow Monitoring Bore	3.21	0.19	14.5	2
		Deep monitoring bore	3.75	0.27	59.0	6
	Sweetwater MW3	Shallow Monitoring Bore	7.36	0.29	5.0	1
		Deep monitoring bore	6.50	0.30	47.0	6
	Sweetwater MW4	Shallow Monitoring Bore	14.64	0.50	25.0	2
		Deep monitoring bore	3.99	0.22	92.0	6
	Sweetwater MW5	Shallow Monitoring Bore	15.67	0.92	6.0	1
		Deep monitoring bore	8.30	0.74	61.0	6
	Sweetwater MW6	Shallow Monitoring Bore	14.45	0.81	15.0	1
	Sweetwater MW7	Shallow Monitoring Bore	15.92	NA	7.0	1
	Sweetwater Nursery	Monitoring bore	5.06	0.43	33.8	3
Lake Heather Monitoring Bores	Lake Heather Piezometer 1	NRC shallow monitoring bore	11.57	0.93	26.0	1
		NRC deep monitoring bore	7.63	0.66	105.5	6
	Lake Heather Piezometer 2	NRC shallow monitoring bore	9.27	0.94	29.5	1
	Lake Heather Piezometer 3	NRC shallow monitoring bore	11.93	0.74	29.0	1

Model Region	Site	Piezometer Description	Mean groundwater level (mAMSL)	Standard deviation (m)	Bore depth (m)	Model Layer
Private Bores in Southern Aupouri Aquifer	Vinac	Private bore	0.04	0.75	33.0	3
	Waipapa	Private bore	2.93	0.14	56.0	4
	Matich	Private bore	4.94	0.18	Unknown	6
	Welch	Private bore	3.25	0.39	31.7	3
	Shanks	Private bore	4.77	0.39	Unknown	2

4.2 Steady-State Calibration

A steady-state model was developed and calibrated to validate the conceptualisation of the groundwater flow model. The objective of the calibration was to obtain approximate values of the model parameters, and to obtain initial heads for transient model simulation. An automated parameter estimation tool, PEST, was used to calibrate hydraulic conductivity and vertical anisotropy of materials for each of the 6 model layers with constraints based on previous modelling studies for the region and literature values. Steady state model outputs were used as a starting point for the transient model calibration process.

For calibration purposes material zones within the model domain were defined vertically based on the model layers described in **Section 3.3** and divided horizontally into four sections along a north-south axis. These zones are shown in **Figure 26** and referred to herein, from north to south as North, Motutangi, Waiharara-Paparore, and South.

Figure 26. Aupouri Aquifer Groundwater Model parameter calibration zones (See A3 attachment at rear).

These divisions were made to enable a model calibration that reflects the fact that the material is heterogeneous and therefore hydraulic characteristics are spatially variable within a given material. The four zones that were defined for the north-south axis were based on geographic areas where groundwater takes are concentrated or where landscape variability was considered likely to indicate variation in hydrogeological characteristics.

Through this method the best possible calibration for the data set was achieved for the setup while ensuring that calibrated parameters were reasonable for the given material types.

The average water levels from 56 piezometers registered on the NRC bore database were used as the calibration targets. The simulated head is plotted against the observations (**Figure 27**).

Changes to the model that were based on the incorporation of LIDAR data were applied directly to the transient model and are therefore not reflected in the steady-state calibration.

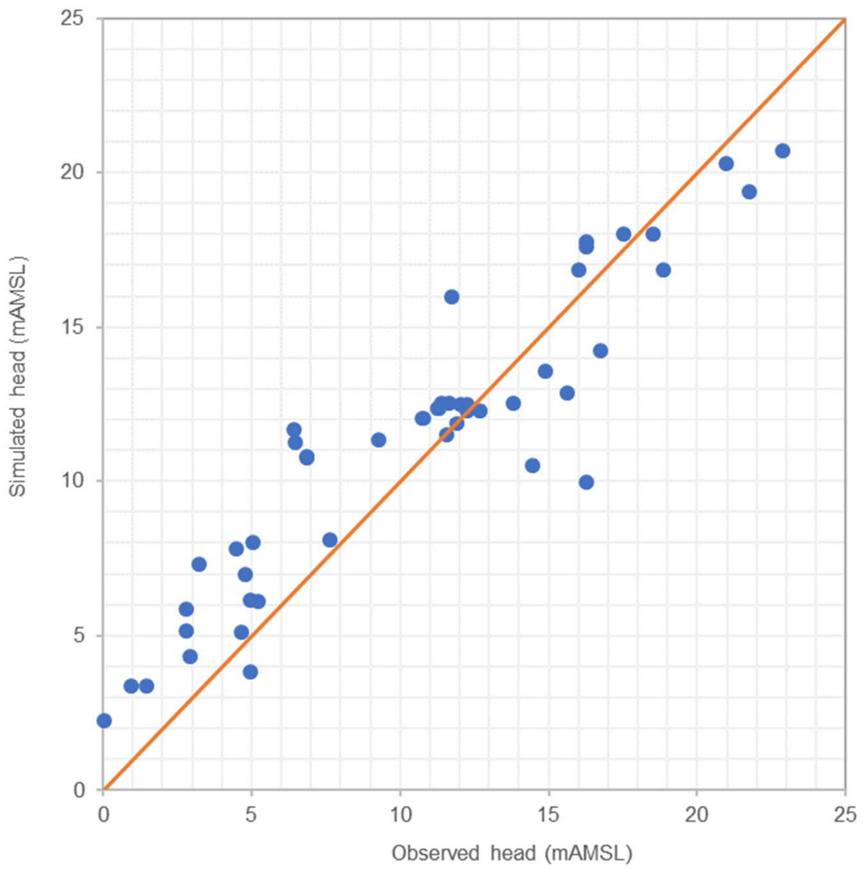

Figure 27. Simulated head versus observed head.

4.3 Transient Calibration

The calibrated parameters from the steady state PEST simulation were used as a starting point for calibrating the transient model. Targeted adjustments were made to hydraulic conductivity, vertical anisotropy, drain elevation, and the conductivity of subsurface boundaries (only on the west coast).

The model was simulated approximately 80 times to obtain a satisfactory calibration. Each transient simulation takes 30 minutes to run, and post processing of results takes 3 minutes, hence a cycle time of approximately 33 minutes is needed for each model simulation. This cycle time enabled a significant number of calibration and sensitivity assessment runs to be undertaken.

After each run, simulated heads from the relevant model layer and cell were extracted and processed with Python code that automatically developed hydrographs and calculated RMSE for each gauge individually, which permitted rapid comparison of simulated versus measured data.

In December of 2020 the results of a LIDAR survey commissioned by NRC became available, constituting an improvement topographic data. Subsequent adjustments were made to hydraulic parameters to improve model calibration from the version completed in 2019.

The transient calibration setup is described in the following sections.

Model Layer	Model Geological Units	Kx		Vertical Anisotropy	Sy	Ss
		(m/d)	(m/s)	(-)	(-)	(m-1)
Layer 1: Interbedded sand, peat, and iron pans	Coastal sand-North	4.20	4.9E-05	8	-	0.30
	Coastal sand-Motutangi	4.85	5.6E-05	56	-	0.30
	Coastal sand-Waiharara-Paparore	2.75	3.2E-05	24	-	0.30
	Coastal sand-South	7.50	8.7E-05	24	-	0.30
	Inland sand-North	2.40	2.8E-05	16	-	0.25
	Inland sand-Motutangi	3.00	3.5E-05	103	-	0.25
	Inland sand-Waiharara-Paparore	1.00	1.2E-05	51	-	0.25
	Inland sand-South	0.60	6.9E-06	85	-	0.25
	Peat wetland-Motutangi	0.12	1.4E-06	12	-	0.05
	Peat-Waiharara-Paparore	1.00	1.2E-05	12	-	0.05
	Estuary-Waiharara-Paparore	1.00	1.2E-05	12	-	0.10
	Plains-South	8.00	9.3E-05	12	-	0.20
Layers 2 & 3: Interbedded sand, peat, and iron pans	Coastal sand-North	4.20	4.9E-05	8	5.0E-04	-
	Coastal sand-Motutangi	4.80	5.6E-05	24	5.0E-04	-
	Coastal sand-Waiharara-Paparore	2.55	3.0E-05	32	5.0E-04	-
	Coastal sand-South	12.00	1.4E-04	32	5.0E-04	-
	Inland sand-North	4.20	4.9E-05	8	5.0E-04	-
	Inland sand-Motutangi	2.00	2.3E-05	72	5.0E-04	-
	Inland sand-Waiharara-Paparore	2.50	2.9E-05	48	5.0E-04	-
	Inland sand-South	0.80	9.3E-06	50	5.0E-04	-
Layer 4: Upper Shellbed	Upper Shellbed-North	36.00	4.2E-04	1	1.1E-03	-
	Upper Shellbed-Motutangi	32.00	3.7E-04	1	1.1E-03	-
	Upper Shellbed-Waiharara-Paparore	15.00	1.7E-04	1	1.1E-03	-
	Upper Shellbed-South	20.00	2.3E-04	1	1.1E-03	-
Layer 5: Compact Sand	Compact sand-North	1.20	1.4E-05	48	1.6E-04	-
	Compact sand-Motutangi	7.20	8.3E-05	29	1.6E-04	-
	Compact sand-Waiharara-Paparore	0.60	6.9E-06	48	1.6E-04	-
	Compact sand-South	1.00	1.2E-05	72	1.6E-04	-
Layer 6: Lower Shellbed	Lower Shellbed-North	36.00	4.2E-04	1	1.1E-03	-
	Lower Shellbed-Motutangi	26.40	3.1E-04	1	1.1E-03	-
	Lower Shellbed-Waiharara-Paparore	25.00	2.9E-04	1	1.1E-03	-
	Lower Shellbed-South	25.00	2.9E-04	1	1.1E-03	-

4.3.1 Stress Periods and Time Steps

The model was simulated in transient mode for 58.6 years from 1/01/1960 to 31/07/2018. The simulation was subdivided into 371 stress periods, where imposed stresses (e.g. recharge and pumping) remain constant. The number of stress periods was selected on the basis of i) temporal variation of the transient dataset values; and ii) computational time. The resulting stress period lengths ranged from 13 to 185 days. Stress periods were locked on 1 October and 30 April in each year for the start and end of the irrigation season, respectively, to ensure the irrigation demands were distributed to the correct timeframe.

Each stress period consisted of five time-steps, with head and flow volume in each model cell evaluated at the end of each time step.

4.3.2 Groundwater Pumping

The estimated historical use dataset described in **Section 2.8.1** was implemented in the calibration simulations.

4.3.3 Initial Conditions

The transient model used the steady-state model heads as the starting condition. During the transient calibration process, the starting heads were re-set periodically as parameters were updated. This enabled the starting condition to better reflect the dynamic head distribution within the model under the imposed set of stresses and resulted in minimisation of rapid fluctuations in simulated levels and flows at the start of the simulation (i.e. increased stability).

4.3.4 Model Parameters

The model was calibrated by adjusting parameters for materials both horizontally and vertically to best simulate groundwater elevations measured at observation bores. The calibrated model parameters are shown in **Table 6**. The calibrated model parameters, where applicable, are consistent with calibrated model parameters used in previous modelling (WWA, 2017; WWA, 2018).

The calibrated model hydraulic conductivity for the upper shellbed aquifer ranges from $1.7x10^{-4}$ m/s in the Waiharara-Paparore region to $4.2x10^{-4}$ m/s in the Northern region. In the lower shellbed aquifer conductivity ranges from $2.9x10^{-4}$ m/s in the Southern and Waiharara-Paprore regions to $4.2x10^{-4}$ m/s in the Northern region. As shown in **Table 2,** these values are within the range of horizontal hydraulic conductivity measured and modelled in the past for both the upper and lower shellbed aquifers (Layer 2 and 4). Similarly, for the various sand units, the calibrated model values range from $1.4x10^{-4}$ m/s to $6.9x10^{-6}$ m/s, which is consistent with the range in previously documented values as shown in **Table 2.** Calibrated hydraulic conductivity in the wetland, estuary and peat zones is somewhat lower in the Motutangi and Waiharara regions.

Table 6. Calibrated model parameters.

4.4 Calibrated Model Output

4.4.1 Groundwater Levels

As previously stated in **Section 2.7**, groundwater levels recorded within 17 NRC monitoring piezometers were used to calibrate the transient groundwater model. **Appendix E** provides hydrographs and water level maps of simulated groundwater levels plotted against observed data for comparison purposes, and calibration results for each observation bore are shown in **Table 7**. The observation bores referenced in **Table 7** are the same as those described in **Section 4.1** and shown in **Figure 5**.

Table 7. Model calibration results at observation bores.

Model Region	Site	Piezometer Description	Root Mean Squared Error	Mean groundwater level (mAMSL)	Bore depth	Model Layer
Hukatere Transect	Waterfront	NRC shallow monitoring bore	0.40	0.94	19.0	2
		NRC middle monitoring bore	0.48	1.47	37.0	2
		NRC deep monitoring bore	1.17	2.81	57.0	3
		NRC deep monitoring bore	0.32	2.78	74.0	4
	Hukatere	NRC shallow monitoring bore	1.78	13.79	19.0	1
		NRC middle monitoring bore	1.05	12.68	36.0	2
		NRC deep monitoring bore	0.78	12.26	58.0	2
	Forest	NRC shallow monitoring bore	1.60	18.51	16.0	1
		NRC middle monitoring bore	1.01	17.53	36.0	1
		NRC deep monitoring bore	0.93	16.26	64.0	2
		NRC deep monitoring bore	0.86	16.25	79.0	3
	Burnage	NRC shallow monitoring bore	4.34	15.61	17.0	1
	Browne	NRC shallow monitoring bore	2.97	18.86	16.0	1
		NRC shallow monitoring bore	0.48	16.00	29.0	1
		NRC deep monitoring bore	3.11	11.72	59.0	2
	Wagener Golf Club	Deep monitoring bore	1.79	4.48	69.0	4
	Fishing Club at Houhora	Deep monitoring bore	0.61	3.65	78.0	5
Waiharara-Paparore Region	Kaimaumau Deep	NRC Monitoring Bore	1.11	2.44	72.0	6
	Ogle Drive	NRC Monitoring Bore	0.72	14.90	68.0	2
	Paparore	NRC deep monitoring bore	0.99	6.88	75.0	6
		NRC deep monitoring bore	0.98	6.88	65.0	6
		NRC middle monitoring bore	1.86	6.46	35.0	2
		NRC shallow monitoring bore	1.90	6.42	18.0	2
	Valic-1	Shallow Monitoring Bore	1.04	21.74	17.0	1

Model Region	Site	Piezometer Description	Root Mean Squared Error	Mean groundwater level (mAMSL)	Bore depth	Model Layer
		Deep monitoring bore	0.86	11.65	103.0	6
		Production Bore	0.92	11.41	103.0	6
	Valic-2	Shallow Monitoring Bore	0.83	22.88	55.0	1
		Deep monitoring bore	1.16	12.24	121.0	6
		Production Bore	0.93	12.06	121.0	6
	Valic-3	Shallow Monitoring Bore	2.20	20.99	45.0	1
		Deep monitoring bore	1.89	11.28	124.0	6
		Production Bore	2.17	11.32	124.0	6
	Valic-4	Shallow Monitoring Bore	0.70	16.75	13.0	1
		Deep monitoring bore	0.71	10.77	93.0	6
		Production Bore	0.69	10.75	93.0	6
Sweetwater Farms Monitoring Wells	Sweetwater MW1	Shallow Monitoring Bore	3.59	16.25	13.3	1
		Deep monitoring bore	2.43	5.22	94.0	6
	Sweetwater MW2	Shallow Monitoring Bore	0.40	3.21	14.5	2
		Deep monitoring bore	0.39	3.75	59.0	6
	Sweetwater MW3	Shallow Monitoring Bore	1.82	7.36	5.0	1
		Deep monitoring bore	1.38	6.50	47.0	6
	Sweetwater MW4	Shallow Monitoring Bore	11.54	14.64	25.0	2
		Deep monitoring bore	0.38	3.99	92.0	6
	Sweetwater MW5	Shallow Monitoring Bore	4.65	15.67	6.0	1
		Deep monitoring bore	0.98	8.30	61.0	6
	Sweetwater MW6	Shallow Monitoring Bore	1.48	14.45	15.0	1
	Sweetwater Nursery	Monitoring bore	1.11	5.06	33.8	3
Lake Heather Monitoring Bores	Lake Heather Piezometer 1	NRC shallow monitoring bore	0.80	11.57	26.0	1
		NRC deep monitoring bore	1.06	7.63	105.5	6
	Lake Heather Piezometer 2	NRC shallow monitoring bore	1.93	9.27	29.5	1
	Lake Heather Piezometer 3	NRC shallow monitoring bore	0.73	11.93	29.0	1
Private Bores in Southern Aupouri Aquifer	Vinac	Private bore	1.86	0.04	33.0	3
	Waipapa	Private bore	0.46	2.93	56.0	4
	Matich	Private bore	0.33	4.94	Unknown	6
	Welch	Private bore	0.60	3.25	31.7	3
	Shanks	Private bore	0.60	4.77	Unknown	2

Summary statistics were calculated for all observations used in model calibration. The mean residual head is 0.18 m showing that there is not a strong bias for the simulations overpredicting or underpredicting observed groundwater levels. The mean of the RMSE for all gauges is 1.31 m, which is 5.0% of the observed range in groundwater head (26.5 m), while the RMSE for all manual observations in the model is 1.48 m, or 5.6% of the range of observations. The latter number reflects a bias for gauges where more data is available whereas the former metric gives equal weight to a gauge with limited data. A simulated RMSE of less than 10% of the measured range is considered a good calibration so both analysis criteria meet this standard.

The Sweetwater MW4A gauge was excluded from these calculations because the observed water levels were an apparent anomaly and did not align with any nearby monitoring bores, and it was therefore not considered in model calibration. It is apparent that this bore is measuring a perched water table that is not replicated in the regional groundwater model. Simulated and observed hydrographs for all monitoring wells used for model calibration are provided in **Appendix E**.

For the inland piezometers along the Hukatere transect in the Motutangi region (e.g. Hukatere and Forest), the trend of simulated groundwater level generally follows the observed groundwater level. The increase in groundwater levels over recent years has been replicated in the simulation, though is less pronounced than in the observed data set.

A potential reason for this is that variations in seasonal recharge rates have changed in response to land use. The groundwater model has been set up with recharge rates that were simulated based on a constant land use over the model period. However, land use changes and the associated spatial distributions of land cover will affect the quantity and quality of water being recharged to the groundwater system. In fact, the plantation forestry felling cycles on the western side of the peninsula may significantly affect the variation of groundwater recharge. In general, compared to bare land, forestry land tends to decrease the groundwater recharge due to increased interception and evapotranspiration.

Changes in land use take time to propagate to the groundwater system. Depending on the climate, geology, intensity and extent of the land use change, recovery of the groundwater system may vary from 3 to more than 20 years (Moore and Wondzell, 2005). In the meantime, this effect on groundwater system is masked by the climate variation.

It is therefore likely that the mismatch in calibration is in fact due to a temporal variation in groundwater recharge in response to land use change. However, detailed historical land cover data was not available. Reconstructing historical land use change would be a separate study in its own right and it was therefore not currently possible within the timeframe and budget of this project scope, to incorporate the transient variability of recharge into the groundwater model to reflect the land use change in the area.

The Browne and Waterfront piezometers are generally well represented by the simulation, with good correlation of seasonal and annual trends, though in some cases, a discrepancy in water level elevation was observed. In some cases, this reflects the fact that piezometers at different depths correspond to the same model layer, for example the screened interval for Browne piezometers 2 and 3 extends to 16 and 29 m BGL, respectively, however both fall within model Layer 1 and therefore reflect the same simulation results.

In the Waiharara-Paparore region data from the Paparore monitoring well simulated in the deep aquifer, however over-simulated in the shallow aquifer, indicating that there is likely a localised variation in permeability effecting the vertical hydraulic gradient that is not captured in the model. This location has been troublesome for previous modelling efforts (SKM, 2007b) including earlier versions of the AAGWM. However, with the LIDAR DEM implemented in the current version of the AAGWM, a significant improvement in simulation results for this area was achieved.

Measured data at all deep aquifer bores at the Valic locations and at Ogle Drive were well represented by the model as evident in the hydrographs provided in **Appendix E**. Simulated groundwater levels at the deep bores in the Valic orchards are generally within 1 m of measured values except Valic-3 where there is a greater discrepancy in earlier data; however, the last 5 years of the measured data set is similar to simulation results.

The monitoring bore at the Kaimaumau Wetland is under-simulated by an average of 1.1 m, meaning the model is conservative in terms of estimated effects calculated at this important coastal location.

Groundwater levels in the shallow monitoring bores at Valic Orchards were also well simulated with the exception of Valic-3 which was over-simulated. A low permeability zone applied in Layer 2 of the model was applied to replicate the vertical hydraulic gradient that is evident in the monitoring data for this area, though it remains likely that the conceptual model does not capture the full geologic complexity.

In the southern portion of the model area the majority of monitoring wells are associated with Sweetwater Farms. There are five locations with paired shallow and deep monitoring piezometers and several additional single monitoring piezometers at Sweetwater Farms, as well as several bores where groundwater level data is collected by private land owners. Many of these data sets are limited in their historic extent.

Simulated vertical hydraulic gradients at Sweetwater Farms were shallower than field observations for monitoring wells (MW) 1, 3, 4 and 5. At MW-4 the shallow piezometer is likely measuring a perched water table based on the groundwater elevation being inconsistent with the general groundwater gradient in the surrounding area. The simulated water table is generally close to observations in the deep monitoring bores, however water levels at the shallow monitoring wells are under-simulated, with the exception of MW-2. This underscores the difficulty of representing the geologic complexity of the region within the constraints of the conceptual model.

The monitoring bore at Sweetwater Nursery, which is known to have artesian conditions, is reasonably well simulated with an average under-simulation of 1.1 m.

4.4.2 Model Flow Budget

Table 8 provides the long-term average water budget for the transient calibration model.

The main input to the model is groundwater recharge at 650,741 m^3/day (238 billion litres per annum) represents 81% of the total inflow.

Discharge from the model is distributed between subsurface coastal discharges, comprised of the:

- constant head in Layer 1 at 275,249 m^3/day (100.5 billion litres per annum) or 34%,;
- GHB in Layer 2 to 6 at 80,743 m^3/day (29.5 billion litres per annum) or 10%; and
- surface water discharges in the form of drains and wetlands at 278,249 m^3/day (101.8 billion litres per annum) accounting for 35% of the model water budget.

Discharge through groundwater pumping which averages 6,401 m^3/day (2.3 billion litres per annum) is a small component (<1%) of the model water budget, which reflects the fact that many of the large groundwater takes within the model were initiated in the last several years of the simulation period whereas the water balance presented in **Table 8** represents an average for the entire simulation period.

At the time of peak irrigation over the simulation period, December 2010, groundwater pumping accounts for 36,571 m^3/day, amounting to 5.3% of the groundwater budget.

Table 8. Average daily mass balance for 58-year simulation from 1/01/1960 to 31/07/2018.

Mass balance	Components	Baseline Model	
		Flow (m^3/d)	Percentage of Flow (%)
Inflow	Storage	149,766	18.7
	CH	158	0.0
	Recharge	650,741	81.3
	Lakes	134	0.0
	Cross Boundary Flow	NA	NA
	Total inflow	800,800	100
Outflow	Storage	159,628	19.9
	Shallow Coastal Discharge (CH)	275,249	34.4
	Wells	6,401	0.8
	Drains/Wetlands (DC)	278,778	34.8
	Deep Coastal Discharge (GHB)	80,743	10.1
	Cross Boundary Flow	NA	NA
	Total outflow	800,799	100
Percentage discrepancy		0.0%	

Note: CH = constant head; GHB = general head boundary; DC = drain cells. Changes in storage are due to the difference in climatic and hence water table conditions between the start and the end of the model run.

5. Conclusions

A numerical groundwater flow model was developed for the Aupouri aquifer of Northland, New Zealand to be used to assess groundwater resources at the basin scale in the context of historic, present and future conditions. The calibrated model is intended to provide a tool for the evaluation of proposed groundwater extractions and its potential impact on both groundwater and surface water. In particular, the model can be used to define the potential impact from seasonal pumping on the aquifer system water budget, aquifer groundwater levels, surface water drain flows, and the position of the saltwater/fresh water interface.

Model Development

The framework for the model was based on a LIDAR survey for surface elevation and a review of all available borelogs, of which 198 were considered reliable enough to inform the development of the model stratigraphy. Geologic material noted in the borelogs was classified into four primary geologic layers; interbedded dune sand and peat, upper shellbed, compact sand, and lower shellbed; with the shellbed representing the aquifer material. The upper strata were sub-divided into three layers to account for the vertical heterogeneity in the material and allow for associated variability in conductivity and anisotropy to enable model calibration. The model layer base elevations were interpolated from the bore log data with the bottom of the lower shellbed being the lower model boundary.

Recharge to the model area was determined through an assessment of historic climate date and soil types processed using the SMWBM tool to develop a time series input based on historic rainfall and PET. Groundwater pumping was determined through an assessment of groundwater allocation over the model area and demand based on historic climate conditions.

Model Calibration

The model was calibrated to a historic dataset that included groundwater level observations measured at 56 locations. Each observation bore was assigned a model layer based on the depth of the bore and corresponding material within the model. A sensitivity analysis was performed to determine that hydraulic conductivity was the most sensitive model parameter, followed by vertical anisotropy.

The model was calibrated by systematically adjusting parameters in both a steady state and transient application to achieve the best possible agreement between simulated and measured water levels while maintaining realistic parameter values. In the case of the steady state simulation the parameter estimation tool, PEST, was used to determine the parameter values that best fit the observed data. These parameters were then used as the basis for the transient calibration.

The transient model was run for a simulation period of 58 years. A mean RMSE for all gauges of 1.31 m was achieved, which was 5.0% of the range of observations and well within the groundwater modelling guidelines for an acceptable regional model of no greater than 10%. The water level elevations and temporal trends were well simulated in the majority of observation bores.

Water Budget

Approximately 687 billion litres of rainfall per year occurs over the Aupouri Aquifer study area highlighted in this report. Groundwater recharge occurs through the percolation of rainfall at an average rate of 238 billion litres per annum, or approximately 34% of rainfall over the study area, accounting for the majority of groundwater inflow. Groundwater outflows occur primarily as discharge to the coasts (130 billion litres per annum) baseflow in streams and agricultural drains (102 billion litres per annum). Groundwater pumping is a small fraction of the overall groundwater budget; however, it has been increasing in recent years as groundwater allocation for agricultural use increases.

At the time of peak irrigation total groundwater abstraction under current conditions accounts for 37 million litres per day (5.3% of the groundwater budget). Annual groundwater abstraction over the historic period used for model development averaged only 2.5 billion litres per year.

6. References

Edwards, M., 1996, Elimination of adaptive grid interface errors in the discrete cell centred pressure equation: Journal of Computational Physics, v. 126, article no. 0143, p. 356–372.

Isaac, M.J. (compiler), 1996: Geology of the Kaitaia area. Institute of Geological & Nuclear Sciences 1:250 000 geological map 1. 1 sheet + 43 p. Lower Hutt, New Zealand. GNS Science.

Lincoln Agritech, 2015. Aupouri Aquifer Review. Consultancy report prepared for Northland Regional Council.

Panday, Sorab, Langevin, C.D., Niswonger, R.G., Ibaraki, Motomu, and Hughes, J.D., 2013, MODFLOW–USG version 1: An unstructured grid version of MODFLOW for simulating groundwater flow and tightly coupled processes using a control volume finite-difference formulation: U.S. Geological Survey Techniques and Methods, book 6, chap. A45, 66 p

SKM, 2007a. Awanui Artesian Aquifer Numerical Modelling. Consultancy report prepared for Northland Regional Council.

SKM, 2007b. King Avocado Orchard Groundwater Take Consent Application (AEE Final). Consultancy report prepared for King Avocado Limited.

SKM, 2010. Sweetwater Station Water Take Hearing - Response to Section 92 request. Consultancy report prepared for Landcorp Farming Limited and Te Runanga O Te Rarawa.

Van Genuchten, M. Th. 1980. A closed-form equation for predicting the hydraulic conductivity of unsaturated soils. Soil. Sci. Soc. Am. J. 44:892—898.

Moore, R., & Wondzell, S. M. (2005). Physical hydrology and the effects of forest harvesting in the Pacific Northwest: a review. JAWRA Journal of the American Water Resources Association, 41(4), 763-784.Mulder, P. J. M. 1983. Rapportage putproef Hoogezand. Dienst Grondwaterverkenning TNO, Delft, OS.83 – 24, 7p.

Mulder, P.J.M. 1983. Rapportage putproef Hoogezand. Dienst Grondwaterverkenning TNO Delft

Williamson Water Advisory (2017). Motutangi-Waiharara Groundwater Model Factual Technical Report. Consultancy report prepared for Motutangi-Waiharara Water User Group.

Williamson Water Advisory (2018). Waiharara-Paparore Groundwater Model Factual Technical Report. Consultancy report prepared for Valic Avocados ltd, Tiri Orchards ltd, Wataview Orchard

Williamson Water Advisory (2018). Sweetwater Farms PB2 Test Pumping Report. Consultancy Report prepared for Sweetwater Farms Limited.

Appendix A. Summary of Aquifer Hydraulic Properties

The following tables summarise hydraulic property values that have been measured and estimated in models across the Aupouri Peninsula from various reports since 2000.

Table A1. Analysis of aquifer test data (Lincoln Agritech, 2015).

Pump	Screen depth	Test name	Lithology	T	B	Kx	S	K'/B'	B'	K'z
	(mBGL)			(m^2/d)	(m)	(m/d)	(-)	(d)	(m)	(m/d)
200048	18.8	Hukatere 1	Sand	60	6.4	9.4	0.0017	0.1475	13.5	2.0
200048	18.8	Hukatere 1	Sand	60	6.4	9.4	0.0107	0.2927	13.5	4.0
200048	18.8	Hukatere 3	Sand	50	6.4	7.8	0.0022	0.1909	13.5	2.6
200048	18.8	Hukatere 3	Sand	62	6.4	9.7	0.0154	0.1909	13.5	2.6
200060	64	Browne	Sand	400	10.4	38.5	0.0004	0.0014	21.2	0.03
200081	31.2	Ogle Drive	Sand	7.4	8.1	0.9	0.0467	0.8771	10.2	8.9
200229	73	Fitzwater	Shell/sand	130	6	21.7	0.0002	0.0001	26.0	0.004
200229	73	Fitzwater	Shell/sand	110	6	18.3	0.0004	0.0004	11.0	0.004
201025	27	Sweetwater	Sand	52	6.3	8.3	0.0004	0.0018	11.0	0.02
201037	27.2	Welch	Sand/shell	9	1.8	5	0.0005	0.0087	11.9	0.1
209606	110.5	King Avo	Shell	305	26	11.7	0.0007	0.0003	15.5	0.004
209606	110.5	King Avo	Shell	370	17	21.8	0.0011	0.0003	15.8	0.005
			Min	7.4	1.8	0.9	0.0002	0.0001	10	0.004
			Mean	135	8.9	13.5	0.0067	0.14	15	1.7
			Max	400	26	38.5	0.0467	0.88	26	8.9

Table A2. Analysis of aquifer test data (HydroGeo Solutions, 2000).

NRC Bore	Depth	Top of screen	Aquifer type	SWL	T	K	S
	(m)	(mBGL)		(mBGL)	(m^2/d)	(m/s)	(-)
43	55	52	Fine sand	9.3	240 - 280	6E-05 to 7.1E-05	-
48	67	19	Med sand	5.3	80 - 300	6.1E-05 to 7.1E-05	0.01-0.001
59 (s)	6	-	Fine sand	2.8	140	5.10E-04	-
59 (d)	55	49	Fine sand	13.4	190	5.30E-05	-
60	60	-	Fine sand	14.9	220 - 850	5.6E-06 to 1.3E-04	-
81	32	31	Fine sand	20.9	12 - 28	1.25E-05 to 2.9E-05	0.07-0.03
152	66	60	Fine sand	30.1	260	8.40E-05	-
184	110	101	Shelly sand	17.2	140 -340	1.7E-05 to 4.2E-05	-
229 (211)	79	70	Shelly sand	2.6	140	2.10E-05	1.4E-04 to 1.8E-03
230	88	63	Shelly sand	4.6	240 - 310	4.3E-05 to 3.3E-05	-

NRC Bore	Depth	Top of screen	Aquifer type	SWL	T	K	S
	(m)	(mBGL)		(mBGL)	(m^2/d)	(m/s)	(-)
1007	50	45	Fine sand	33.7	275 -305	2.1E-04 to 1.9E-04	-
1025	30	27	Fine sand	1.55	60 -103	2.2E-05 to 3.7E-05	2.5E-04 to 5.0E-04
1374	32	26.6	Fine sand	0.8	48	1.80E-05	1.0E-05 to 2.0E-05
1424*	82	70	-	-	260	-	-

Table A3. Summary of aquifer test data (SKM, 2010).

Bore Owner	Well ARC No	Easting (NZMG)	Northing (NZMG)	Test Type	Test Dur. (hrs)	Rate (m^3/day)	Obs. Bores	Screen Geology	K (m/s)	Information Source
King	201374	2533400	6681500	Constant Rate	24	576	Yes (1)	Shell	1.8E-05	HydroGeo Solutions (2000)
Sweetwater Orchards	201424	2529558	6684434	Constant Rate	72	1,176	Yes (1)	Shell	1.9E-04	Woodward Clyde (1998)
Kaurex Corporation	200230	2530331	6697328	Constant Rate	9.5	273	No (PB only)	Shell	4.3 – 3.3E-05	HydroGeo Solutions (2000)
Matai Orchards	201507	2529399	6691299	Constant Rate	88.5	497	Yes (1)	Shell	4.0 – 2.0E-04	SKM (2007)
Hopkins	200184	2520300	6706800	Constant Rate	24	260	No (PB only)	Shell	4.2 – 1.7E-05	HydroGeo Solutions (2000)
Fitzwater	200229	2529743	6690648	Constant Rate	24	864	Yes (4)	Shell	2.1 – 1.4E-04	HydroGeo Solutions (2000) and SKM (2007)
Brown	200060	2521699	6706300	Constant Rate	22	708	Yes (3)	Sand	5.6E-06 – 1.3E-04	HydroGeo Solutions (2000)
Hogg	201007	2528300	6685799	Constant Rate	20.9	160	No (PB only)	Sand	2.1 – 1.9E-04	HydroGeo Solutions (2000)
Waiharara	209499	2528580	6690100	Constant Rate	91	1,113	Yes (2)	Shell	2.0E-04	SKM (2007)
King Avocado Ltd	209606	2527482	6690562	Constant Rate	168	2,393	Yes (3)	Shell	4.3 – 1.5E-04	SKM (2007)
Hamilton Nurseries	201025	2531401	6684155	Constant Rate	6	300	Yes (2)	Sand	1.2E-04	SKM (2001)
Stanisich Orchard	200192	2528600	6695799	Constant Rate	1	1,442	No (PB only)	Shell	5.0E-05	SKM (2002a)
Terra Nova Orchard	200335	2521199	6706499	Constant Rat	39	674	Yes (6)	Shell	4.0 – 3.0E-04	SKM (2002b)
Northland Catchment Commission	200048	2519855	6701857	N/A	N/A	N/A	N/A	Sand	7.1 – 6.1E-05	HydroGeo Solutions (2000)
Northland Catchment Commission	200081	2528583	6689795	N/A	N/A	N/A	N/A	Sand	2.9 – 1.25E-05	HydroGeo Solutions (2000)

Colville	200059	2521792	6705887	Step (4)	22.3	63 - 233	No (PB only)	Sand	5.3E-05	HydroGeo Solutions (2000)
Fraser	201002	2525552	6671053	Step (3)	22	89 - 163	No (PB only)	Sand	3.0E-04	NRC database
Richards Enterprises	200043	2522513	6708792	Step (4)	19	149 -333	No (PB only)	Sand	7.1 – 6.0E-05	HydroGeo Solutions (2000)
Herbert	200152	2528178	6688977	Step (4)	20	127 - 319	No (PB only)	Sand	8.4E-05	HydroGeo Solutions (2000)

Table A4. Calibrated model parameters (SKM, 2007a).

Material ID	Hydraulic Conductivity		Vertical anisotropy	Sy
	(m/d)	(m/s)	(-)	(-)
Loose dune sand	10	1.20E-04	10	0.2
Weathered dune sand	6	6.90E-05	10	0.2
Fine sand	3	3.50E-05	25	0.25
Peat and sand	0.1	1.20E-06	30	0.2
Upper alluvium	0.55	6.40E-06	10	0.3
Alluvium	0.06	6.90E-07	20	0.05
Shellbed	50	5.80E-04	2	0.3

Table A5. Aquifer hydraulic parameters derived from SKM102PB test pumping (SKM, 2007b).

Bore	T	K	
	(m^2/s)	(m/d)	(m/s)
SKM101b	3.70E-03	32	3.70E-04
SKM102b	1.50E-03	13	1.50E-04
SKM103b	3.50E-03	30	3.50E-04
SKM104b	4.30E-03	37	4.30E-04

Table A6. Material parameters used within PLAXIS geotechnical subsidence model (SKM, 2007b).

King Avocado Orchard Groundwater Take Consent Application (AEE Final)							
Material	Density (KN/m$^{3)}$		Permeability (m/d)		Stiffness (kN/m^2)	Cohesion (kN/m^2)	Friction Angle (°)
	δunsat	δsat	Kx	Ky	E50ref	cref	ø
Loose Dune Sand	15	17	5	0.25	10000	0.2	28

Compact Dune Sand	17	19	0.7	0.07	15000	0.2	28
Shellbed	18	20	22	2.2	30000	1	30

Table A7. Hydrogeological data calculated from pumping tests (WWA, 2017).

Farm	Rate (L/s)	Bore	Screen Depth (mBGL)	Method	T (m^2/d)	S (-)	B (m)	K (m/d)	K (m/s)
Stanisich Farm	25	Pumping bore	87-101	Single well Jacob	485	-	14	35	4.1E-04
				Theis Recovery	512	-		37	4.3E-04
	-	Monitoring bore	77-85	Theis (point match)	356	0.0044	8	45	5.2E-04
Honeytree Farm	29	Pumping bore	62-68, 68-71,84-93	Single well Jacob	618	-	18	34	3.9E-04
				Theis Recovery	511	-		28	3.2E-04
	-	Monitoring bore	63-69, 69-72,86-95	Theis (point match)	751	0.0003	18	42	4.9E-04
				Cooper Jacob	784	0.0003		44	5.1E-04
De Bede Farm	2.3	Pumping bore	91-97	Single well Jacob	377	-	6	63	7.3E-04
				Theis Recovery	363	-		61	7.1E-04
				Max	784	0.0044		63	7.3E-04
				Min	356	0.0003		28	3.2E-04
				Mean	528	0.0016		43	5.0E-04

Table A8. Calculated hydrogeological property from Single well Jacob method (WWA, 2017).

Farm	Q (L/s)	Bore	Screen Depth (mBGL)	Evaluation time (s)	T (m^2/d)	B (m)	K (m/d)	K (m/s)	Time (s) evaluation criteria	
									Minimum	Maximum
Stanisich	25	Pumping bore	87-101	210 - 1200	471	14	34	3.9E-04	183	1728
De Bede	2.3	Pumping bore	91-97	330 - 1470	273	6	46	5.3E-04	86	1728

Table A9. Estimated hydrogeological parameters from Hantush – Jacob method (WWA, 2017).

Bore	T	K_h	K_h	K'/B'	S_s
	m^2/d	m/d	m/s	d^{-1}	m^{-1}
Stanisich observation bore 2 (monitoring bore)	138	10	1.14E-04	1.83E-03	1.55E-04
	408	29	3.38E-04	1.35E-03	3.07E-04
	348	25	2.88E-04	7.36E-04	3.13E-04
Honeytree farm production bore 1(monitoring bore)	579	32	3.72E-04	1.50E-04	1.63E-05
	484	27	3.11E-04	2.84E-04	2.17E-05
	707	39	4.54E-04	5.09E-05	1.70E-05

Table A10. Calibrated Model Parameters (WWA, 2017).

Model Geological Units	Model Layer	K_x		Vertical Anisotropy	S_y	S_s
		(m/d)	(m/s)	(-)	(-)	(m^{-1})
Coastal sand	1	4.5	5.2E-05	70	0.3	-
Weathered sand	1	2.8	3.2E-05	90	0.25	-
Plain zone	1	0.1	1.2E-06	15	0.01	-
Coastal sand	2&3	4	4.6E-05	30	-	0.0005
Weathered sand	2&3	3	3.5E-05	80	-	0.0005
Shellbed	4	35	4.1E-04	1	-	0.0016
Sand	5	6	6.9E-05	30	-	0.0005
Shellbed	6	22	2.5E-04	1	-	0.0016

Table A11. Test pumping results for Sweetwater Farms (WWA, 2018).

Test	Analysis	Pumping rate		Screen length	Transmissivity (T)	Hydraulic conductivity (K)	Specific storage (/m)
		L/s	m^3/d	m	m^2/d	m/s	
Constant pumping	PB6 Cooper-Jacob	64	5,495	17	5,700	3.9E-03	9.6E-04
	PB2 Cooper-Jacob	64	5,495	17	430	2.9E-04	-
Recovery	PB2 Theis	64	5495	17	354	2.4E-04	-

Appendix B. Recharge Modelling

B.1 Model Parameters

The soil moisture water balance model (SMWBM) is a deterministic lumped parameter model originally developed by Pitman (1976) to simulate river flows in South Africa. The code was reworked into a Windows environment and the functionality extended to include a surface ponding function, additional evaporation functions and an irrigation module.

The model utilises daily rainfall and potential evaporation data to calculate soil moisture conditions and the various components of the catchment water balance under natural rainfall or irrigated conditions. The model operates on a time-step with a maximum length of daily during dry days, with smaller hourly time-steps implemented on wet days.

The model incorporates parameters that characterise the catchment in terms of:

- interception storage,
- evaporation losses,
- soil moisture storage capacity,
- plant available water capacity,
- soil infiltration,
- sub-soil drainage;
- vadose zone vertical drainage'
- surface runoff (quickflow);
- stream baseflows (groundwater contribution); and
- the recession and/or attenuation of groundwater and surface water flow components, respectively.

B.2 Fundamental Operation

The fundamental operation of the model is as follows and in **Table B1**:

When a rainday occurs, daily rainfall is disaggregated into the hourly time-steps based on a pre-defined synthetic rainfall distribution, which includes peak intensities during the middle of the storm. This time stepping approach ensures that rainfall intensity effects and antecedent catchment conditions are considered in a realistic manner by refined accounting of soil infiltration, ponding and evaporation losses.

Rainfall received must first fill a nominal interception storage (PI – see below) before reaching the soil zone, where the net rainfall is assessed as part of the runoff/infiltration calculation.

Water that penetrates the soil fills a nominal soil moisture storage zone (ST). This zone is subject to evapotranspiration via root uptake and direct evaporation (R) according to the daily evaporation rate and current soil moisture deficits. The soil moisture zone provides a source of water for deeper percolation to the underlying aquifer, which is governed by the parameters FT and POW.

If disaggregated hourly rainfall is of greater intensity than the calculated hourly infiltration rate (ZMAX, ZMIN) surface runoff occurs. Surface runoff is also governed by two other factors, which are the prevailing soil moisture deficit and the proportion of impervious portions of the catchment directly linked to drainage pathways (AI).

Rainfall of sufficient intensity and duration to fill the soil moisture storage results in excess rainfall that is allocated to either surface runoff or groundwater percolation depending on the drainage and slope characteristics of the catchment (DIV).

Finally, the model produces daily summaries of the various components of the catchment water balance and calculates the combined surface runoff/percolation to groundwater to form a total catchment discharge.

Table B1. Summary of SMWBM parameters and value assignments for this study.

Parameter	Name	Parameter Values			Description
		Coastal sand	Weather-ed sand	Plain zone	
ST (mm)	Maximum soil water content.	178.5	178.5	100	ST defines the size of the soil moisture store in terms of a depth of water. ST is approximately equivalent to root zone depth divided by soil porosity.
SL (mm)	Soil moisture content where drainage ceases.	0	0	0	Soil moisture storage capacity below which sub-soil drainage ceases due to soil moisture retention.
ZMAX (mm/hr)	Maximum infiltration rate.	20	20	5	ZMAX and ZMIN are nominal maximum and minimum infiltration rates in mm/hr used by the model to calculate the actual infiltration rate ZACT. ZMAX and ZMIN regulate the volume of water entering soil moisture storage and the resulting surface runoff. ZMIN is usually assigned zero. ZMAX is usually assigned the saturated infiltration rate from field testing. ZACT may be greater than ZMAX at the start of a rainfall event. ZACT is usually nearest to ZMAX when soil moisture is nearing maximum capacity.
ZMIN (mm/hr)	Minimum infiltration rate.	0	0	0	
FT (mm/day)	Sub-soil drainage rate from soil moisture storage at full capacity.	5	3.8	0.8	Together with POW, FT (mm/day) controls the rate of percolation to the underlying aquifer system from the soil moisture storage zone. FT is the maximum rate of percolation through the soil zone.
POW (>0)	Power of the soil moisture-percolation equation.	2	2	2	POW determines the rate at which sub-soil drainage diminishes as the soil moisture content is decreased. POW therefore has significant effect on the seasonal distribution and reliability of drainage and hence baseflow, as well as the total yield from a catchment.
AI (-)	Impervious portion of catchment.	0	0	0.01	AI represents the proportion of impervious zones of the catchment directly linked to drainage pathways.
R (0,1,10)	Evaporation-soil moisture relationship	0	0	0	Together with the soil moisture storage parameters ST and SL, R governs the evaporative process within the model. Three different relationships are available. The rate of evapotranspiration is estimated using either a linear (0,1) or power-curve (10) relationship relating evaporation to the soil moisture status of the soil. As the soil moisture capacity approaches full, evaporation occurs at a near maximum rate based on the mean monthly pan evaporation rate, and as the soil moisture capacity decreases, evaporation decreases according to the predefined function.
DIV (-)	Fraction of excess rainfall allocated directly to pond storage.	0	0	0	DIV has values between 0 and 1 and defines the proportion of excess rainfall ponded at the surface due to saturation of the soil zone or rainfall exceeding the soils infiltration capacity to eventually infiltrate the soil, with the remainder (and typically majority) as direct runoff.
Kv (m/s)	Vertical hydraulic conductivity	8E-6	5E-6	2E-8	Kv along with the VGn parameter and the soil moisture status governs the unsaturated hydraulic conductivity and travel times within the vadose zone.

Parameter	Name	Parameter Values			Description
		Coastal sand	Weather-ed sand	Plain zone	
VGn (-)	van Genuchten parameter	2.68	2.68	1.09	Defines the soil moisture to unsaturated conductivity relationship according to van Genuchten's equation.
VPor (-)	Average porosity of the vadose zone	0.15	0.15	0.40	This is typically fixed and not changed during calibration as changes can easily be compensated for in Kv.
D (m)	Average depth of the vadose zone	10	10	1	The deeper the vadose zone, the longer the travel times.
TL (days)	Routing coefficient for surface runoff.	1	1	1	TL defines the lag of surface water runoff. This is not necessary to define for this study as we are only interested in the groundwater percolation component of the water balance.
GL	Groundwater recession parameter.	1	1	1	GL governs the lag in groundwater discharge or baseflow from a catchment.

B.3 Vadose zone discharge functionality

Based on the simulated groundwater percolation from the soil moisture model, the vadose zone discharge functionality was utilised to simulate the vertical movement of water in the unsaturated zone. The depth and hydraulic properties of the vadose zone govern the delay in groundwater response to climate variation.

The vadose zone functionality built into the SMWBM is premised on three principals:

1. ***Unsaturated hydraulic conductivity -*** The van Genuchten (1980) equation was used to determine unsaturated hydraulic conductivity in the vadose zone, which is governed by the saturated hydraulic conductivity that sets the upper value, and the degree of saturation in the soil zone as a proxy for general sub-surface degree of wetness.

2. ***Vertical flux rate*** - The simplified Richard's equation is used to estimate the vertical flux rate of water, which is assumed to be driven by gravitational force (only) and therefore governed by unsaturated hydraulic conductivity and porosity.

3. ***Transport time*** - The Muskingum equation was used to translate the vertical flux into a routing scheme, using the depth of the vadose zone and vertical flux rate (velocity) as the time component of the equation.

The delay in groundwater recharge was observed for coast sand, weathered sand and peat and clay to different extents. The simulated results for weathered sand suggest that the groundwater recharge has approximately 2-3 months delay in responding to the rainfall variation, depending on locality. **Figure B1.** provides an example of the functionality of the vadose zone model.

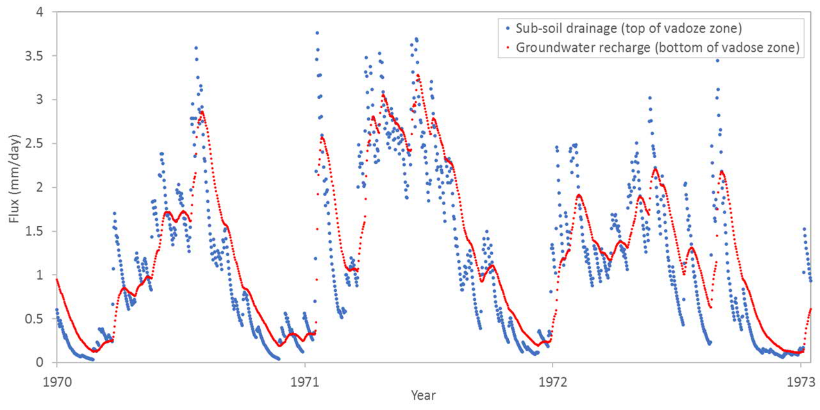

Figure B1. Graph comparing inputs and outputs from vadose zone model.

Appendix C. Groundwater Takes

All groundwater takes incorporated in the model are listed in **Table C1** through **Table C3**. Bores with figure reference identification numbers beginning with "C" are for bores with a consented groundwater take. Bores with figure reference identification numbers beginning with "P" are for bores with a proposed groundwater take.

Table C1. Consented and proposed groundwater users in Northern portion of the model corresponding to Figure 9A

Figure reference	IRISID (where available)	Bore Owners	Groundwater Take- Consented Total (m³/yr)	Groundwater Take per Bore (m³/yr)	X coordinate	Y coordinate
C1	AUT.007669.01.02	Rarawa campground	8,036	8,036	1607445	6157509
C2	AUT.017428.01.02	Henderson Bay Avocados-Consented	13,000	13,000	1605547	6154694
C3	AUT.015147.01.03	Thomas & OConnor-Waihopo	98,000	98,000	1604154	6154613
C4	AUT.012071.01.01	Waikopu Avocados-Consented	44,640	44,640	1604046	6153129
C5	AUT.037987.01.01	Walker & MacMillan	40,000	40,000	1602904	6152422
C6	AUT.029091.01.01	G J & D J Price	7,500	7,500	1606898	6152070
C7	AUT.003768.01.04	L & P Trust	6,000	6,000	1606061	6149936
C8	AUT.039244.01.01	Kelvin Thomas*	59,600	59,600	1610222	6147542
C9	AUT.037292.01.01	Fullam GW take	14,000	14,000	1609975	6147378
C10	AUT.039381.01.01	Brien Lamb*	14,900	14,900	1610058	6147313
C11	AUT.040369.01.01	Thomas & OConnor-Houhora	4,500	4,500	1609919	6147193
C12	AUT.002890.01.02	LL & DF Rasmussen	43,200	43,200	1611481	6146609
C13	AUT.004543.01.03	Wagener Houhora Heads Properties Ltd	45,000	45,000	1612372	6145137
C14	AUT.003883.01.03	Longbeach Trust	26,400	26,400	1610973	6145083
C15	AUT.003841.01.02	Tomo Orchard Ltd	14,800	14,800	1610945	6144743
C16	AUT.008203.01.02	Ongare Trust-2	37,200	37,200	1611610	6144688
C17	AUT.026611.01.01	Alligator Pear Partnership	49,752	49,752	1611191	6144687
C18	AUT.039345.01.01	McLarnon-Ongare trust*	23,520	23,520	1611284	6144679
C19	AUT.012472.01.01	Ongare Trust-1	17,856	17,856	1611345	6144535
C20	AUT.009808.01.02	B C Smith	51,200	51,200	1610575	6144488
C21	AUT.020726.02.02	E J Williams	33,000	33,000	1610309	6144289
C22	AUT.028511.01.02	Far North Avos Limited	32,000	32,000	1610547	6144269
C23	AUT.020727.02.02	Honeytree Farms Ltd	33,000	33,000	1610360	6144161
C24	AUT.023557.01.02	Whispering Pines Ltd	46,000	46,000	1611525	6144087
C25	AUT.003726.01.02	Hine & Associates current	74,400	74,400	1610798	6144048
C26	AUT.008605.01.02	Trebcombe Limited-1	52,080	52,080	1611216	6143980
C27	AUT.007735.01.04	S127 GW take	66,000	66,000	1610514	6143937
C28	AUT.038075.01.01	McQuarrie	12,000	12,000	1611559	6143858
C29	AUT.003527.01.02	Trebcombe Limited-2	26,040	26,040	1610842	6143760
C30	AUT.003888.01.02	RB Freeman-1	34,560	34,560	1611320	6143725

Figure reference	IRISID (where available)	Bore Owners	Groundwater Take- Consented Total (m^3/yr)	Groundwater Take per Bore (m^3/yr)	X coordinate	Y coordinate
C31	AUT.008586.02.01	EJ Wagener	30,000	30,000	1611836	6143656
C32	AUT.007108.01.02	Matalaka Trust	16,740	16,740	1610610	6143652
C33	AUT.003372.01.02	RB Freeman-2	25,920	25,920	1610829	6143550
C34	AUT.037274.01.01	Whalers Rd Houhora	74,500	74,500	1611997	6143025
C35	AUT.036910.01.02	Soltysik-Freeman Fam Trust	135,000	135,000	1611801	6142975
C36	AUT.038732.01.01	Valadares*	22,350	22,350	1611872	6142927
C37	AUT.040174.01.01	Mapua Avocados-1	627,000	209,000	1612784	6142645
C38		Mapua Avocados-2		209,000	1612979	6142360
C39		Mapua_Avocados-3		209,000	1612541	6141795
C40	AUT.008340.01.03	Shirttail Orchards	158,520	158,520	1613554	6140038
C41	AUT.003964.01.03	Subritzky	67,106	67,106	1614010	6139855
C42	AUT.038379.01.01	De Bede	70,000	70,000	1615069	6139351
C43	AUT.039332.01.01	L J King*	78,400	78,400	1614723	6139203
C44	AUT.038589.01.01	Thompson*	35,280	35,280	1614798	6138773
C45	AUT.008647.01.03	Avokaha Ltd	31,200	31,200	1614554	6138575
C46	AUT.038591.01.01	Cypress Hills Ltd1*	35,280	35,280	1614898	6138495
C47	AUT.028834.01.01	JR Avocados Ltd	20,000	20,000	1614800	6138422
C48	AUT.038410.01.00	GT&MT Covich-1*	223,500	111,750	1617353	6136859
C49		GT&MT Covich-2*		111,750	1617128	6136793
C50	AUT.038471.01.02	Honeytree2	346,426	173,213	1618611	6136321
C51		Honeytree1*		173,213	1618903	6136060
C52	AUT.038513.01.01	Ngai Takakto1*	193,700	96,850	1618987	6135795
C53		Ngai Takakto2*		96,850	1619097	6135520
C54	AUT.017559.02.01	IJ & BM Broadhurst	105,000	105,000	1619399	6134994
C55	AUT.016914.02.01	I M Fulton-2	40,000	40,000	1619585	6134880
C56	AUT.029171.01.01	J P Broadhurst	24,000	24,000	1619442	6134796
C57	AUT.038380.01.01	Holloway*	14,900	14,900	1619702	6134754
C58	AUT.029109.01.01	I M Fulton-1	20,000	20,000	1619452	6134520
C59	AUT.038328.01.01	KB&SD Shine*	39,200	39,200	1619411	6134224
C60	AUT.038454.01.01	Elbury Holdings-King*	113,700	113,700	1619850	6133782
C61	AUT.027391.01.01	Stanisich-1	120,000	120,000	1618046	6133608
C62		Stanisich-2	64,070	64,070	1617846	6133480
C63	AUT.038420.01.01	Largus-2*	193,700	96,850	1618156	6132087
C64		Largus-1*		96,850	1617905	6132480
C65	AUT.038650.01.01	Hewitt*	39,200	39,200	1617436	6132318
C66	AUT.038339.01.01	Broadhurst	50,000	50,000	1618994	6131326
C67	AUT.020533.02.01	Luca Vista	24,200	24,200	1619057	6130879
C68	AUT.038402.01.01	Bell	35,000	35,000	1619211	6130581
C69	AUT.036868.01.01	Stanisich2	60,000	60,000	1618376	6129421

Figure reference	IRISID (where available)	Bore Owners	Groundwater Take- Consented Total (m^3/yr)	Groundwater Take per Bore (m^3/yr)	X coordinate	Y coordinate
C70	AUT.003580.01.03	Rangaunu	35,000	35,000	1618726	6129089
C71	AUT.017045.01.02	Valic-1	558,000	186,000	1617061	6128196
C72		Valic-2		186,000	1616610	6128425
C73		Valic-3		186,000	1616982	6128849
C74	AUT.004564.01.04	Far North Farms Ltd	80,000	80,000	1618816	6128564
C75	AUT.003968.01.03	DG&HA Inglis	25,000	25,000	1618916	6128385
C76	AUT.014520.02.01	Millpara	183,920	91,960	1617699	6128150
C77		Millpara		91,960	1617696	6127997
C78	AUT.002459.01.03	Avocado Investments Ltd	18,600	18,600	1617322	6126681
C79	AUT.008589.01.02	RA&LS Huddart	11,040	11,040	1617926	6126666
C80	AUT.003788.01.03	Javo	18,600	18,600	1617131	6126650
C81	AUT.004350.01.03	Hayward	24,000	24,000	1618191	6126546
C82	AUT.008177.01.02	JB & GM Clark	24,000	24,000	1618190	6126545
C83	AUT.003798.01.04	NG Rouse	16,500	16,500	1617423	6126357
C84	AUT.028476.01.01	J Jones	60,000	60,000	1618328	6125903
C85	AUT.004571.01.03	DC&MA Olsen	45,000	45,000	1619564	6125618
C86	AUT.007618.01.03	Te Urungi O Ngati Kuri LTD	18,250	18,250	1623319	6122860
C87	AUT.003606.01.04	Far North Holiday Park-Non irrigation	10,920	10,920	1615677	6122797
C88	AUT.008391.01.02	J A Trussler	148,800	148,800	1618833	6122488
C89	AUT.025683.01.03	FNDC: GW take for Kaitaia-1	1,460,000	730,000	1618250	6121600
C90		FNDC:_GW_take_for_Kaitaia-2		730,000	1618307	6121233
C91	AUT.010649.01.03	Landcorp Farming Limited	200,000	200,000	1619617	6120296
C92	AUT.020995.01.03	Sweetwater-1	2,317,000	598,000	1617473	6119002
C93		Sweetwater-2		508,760	1617846	6119771
C94		Sweetwater-Other consented bores		110,022	Multiple locations	
C95	AUT.007148.01.02	KJ & FG King : GW for Awanui Straight-1	278,262	92,754	1622335	6119515
C96		KJ & FG King : GW for Awanui Straight-2		92,754	1622954	6119131
C97		KJ & FG King : GW for Awanui Straight-3		92,754	1622365	6119515
C98	AUT.007429.01.03	RF & MH Barber-Tudorwood Orchard	23,760	23,760	1623509	6117021
C99	AUT.016645.01.02	Landcorp-domestic	21,900	21,900	1616796	6112202
C100	AUT.002898.01.03	Fraser-Ahipara	10,000	10,000	1614673	6109021
P1	APP.017428.02.01	Henderson Bay Avocados	19,000	19,000	1605623	6154872
P2	APP.040600.01.01	Far North Avocados (Blake Powell)	32,000	32,000	1605981	6154581
P3	APP.040601.01.01	Waikopu Avocados	83,360	83,360	1603347	6153388

Figure reference	IRISID (where available)	Bore Owners	Groundwater Take- Consented Total (m^3/yr)	Groundwater Take per Bore (m^3/yr)	X coordinate	Y coordinate
P4	APP.039859.01.01	Te Raite Station-Waihopo	1,170,000	60,000	1605333	6151462
P5		Te Raite Station-Other		175,000	1603898	6151179
P6		Te Raite Station-Waihopo		60,000	1607102	6150752
P7	APP.041211.01.01	P McGlaughlin	78,400	78,400	1606049	6150294
P8	APP.040231.01.01	P&G Enterprises	28,000	28,000	1609182	6148952
P9	APP.039859.01.01	Te Raite Station-Houhora	1,170,000	175,000	1608383	6148854
P10	APP.040121.01.01	J Evans	160,000	160,000	1609492	6148850
P11	APP.039859.01.01	Te Raite Station-Houhora	1,170,000	180,000	1609287	6148271
P12	APP.040652.01.01	S. & L. Blucher	96,000	96,000	1610145	6148091
P13	APP.039859.01.01	Te Raite Station-Houhora	1,170,000	110,000	1607182	6148084
P14		Te Raite Station-Houhora		110,000	1607771	6147949
P15		Te Raite Station-Houhora		100,000	1609016	6147852
P16		Te Raite Station-Houhora		100,000	1609296	6147373
P17		Te Raite Station-Houhora		100,000	1609655	6147078
P18	APP.040397.01.01	A. Matthews	12,000	12,000	1611038	6146087
P19	APP.039644.01.01	D. Wedding & Doody	304,000	304,000	1610297	6145328
P20	APP.040979.01.01, APP.040777.01.01	M Evans	162,400	162,400	1610554	6145121
P21	APP.040919.01.01	Bryan Esate-1	80,000	80,000	1613415	6143424
P22	APP.040918.01.01	Bryan Esate-2	160,000	160,000	1613901	6142132
P23	APP.039628.01.02	KSL Ltd	30,000	30,000	1614333	6138477
P24	APP.040130.01.01	Tuscany Avocados	36,000	36,000	1614490	6138367
P25	APP.040386.01.01	Robert Campbell	360,000	360,000	1615813	6135787
P26	APP.039841.01.02	Yelavich	52,000	52,000	1616833	6133996
P27	APP.040363.01.01	Wataview	33,750	33,750	1619441	6131282
P28	APP.040361.01.01	Tiri	581,250	290,625	1618056	6130290
P29		Tiri		290,625	1618856	6130196
P30	APP.040362.01.01	Valic-4	173,700	173,700	1617589	6129130
P31	APP.040364.01.01	Ellbury Holdings-Sweetwater-1	200,000	100,000	1618632	6121353
P32		Ellbury Holdings-Sweetwater-2		100,000	1618554	6121002
P33	APP.020995.01.04	Sweetwater-3	776,000	385,000	1617109	6120717
P34		Sweetwater-4		180,000	1616465	6120787
P35		Sweetwater-5		180,000	1617267	6121591
P36		Sweetwater-6		180,000	1616868	6120002
P37		Sweetwater-7		180,000	1617043	6118433
P38		Sweetwater-8		180,000	1616978	6116808
P39		Sweetwater-9		180,000	1617279	6117495
P40		Sweetwater-10		105,000	1617702	6114717
P41		Sweetwater-11		105,000	1617254	6113920
P42		Sweetwater-12		116,667	1616055	6112008

Figure reference	IRISID (where available)	Bore Owners	Groundwater Take- Consented Total (m^3/yr)	Groundwater Take per Bore (m^3/yr)	X coordinate	Y coordinate
P43		Sweetwater-13		116,667	1616563	6111903
P44		Sweetwater-14		116,667	1616889	6111890

*Members of the Motutangi Water Users Group. Applications have been consented but are unexercised as of the completion of this report.

Appendix D. Irrigation Scheduling and Actual Irrigation Use

D.1 Development of an irrigation scheduling dataset

The irrigation module of Soil Moisture Water Balance Model was utilised to optimise irrigation applications for avocado orchards in the area and to provide input into the transient irrigation scenario for groundwater modelling purposes. The parameters and associated values used in the model are shown in **Table C1**.

Table C1. Summary of parameters used in the irrigation model

Parameter	Description	Values	Basis of Values
Maximum Soil Moisture Content (ST)	The capacity of water in mm in the soil at field capacity.	178.5	Estimated from potential rooting depth (PRD) and macroporosity (n). ST = PRD x n/100. 1190 mm x 15%= 178.5 mm
Plant Available Water (PAW)	The amount of water physically accessible by the plants in the root zone in mm.	125	Table 22 of Crop Evapotranspiration - Guidelines for Computing Crop Water Requirements from the Food and Agricultural Organisation of the United Nations (FAO)[1] states that 70% of Total Available Soil Water (interpreted as equivalent to ST in the SMWBM) can be depleted before the point where avocado trees suffer stress. Therefore, PAW = 0.7 x ST
Allowable Deficit (AD)	Soil moisture level where irrigation ceases.	90% of PAW	The avocado is very flood-sensitive with even short periods of waterlogging resulting in reduced shoot growth, altered mineral uptake and root death. To avoid flooding and surface runoff, soil moisture levels during irrigation should not exceed 90% of field capacity.
Minimum/ Critical Deficit (CD)	Percentage of PAW at which further drying of soil would start to have an impact on plant growth rates, and hence CD represents the soil moisture level at which irrigation commences.	40% of PAW	The rule of thumb for critical deficit is 50% of PAW. However, a grower aiming to maximise crop yield may want a small critical deficit of only 20% (80% PAW)[2]. A balance is also required between a small critical deficit (high soil moisture levels) and water wastage, which results under high moisture conditions when rainfall occurs during summer. Through trial and error, we have used CD values of 40% PAW.
Peak Application Depth	Maximum daily irrigation depth applied to soil (mm/day).	4.0 mm	Selected through optimisation target of minimisation in losses, while maintaining moisture levels at or above the CD. Note. This is the amount of irrigation water reaching the soil surface, which is less that the amount applied by the irrigator *per se*. due to application inefficiencies (losses).
Application Duration	Duration in hours over which the peak application depth is applied	2 hours	Data estimated
Rain Threshold	Daily rainfall total in mm when a farmer would choose not to irrigate.	10 mm	Judgement
Season	Irrigation season start and finish	October – April	General irrigation season length.

The historical rainfall record from 01/01/1960 to 31/07/2018 was used in the model. The simulated soil moisture content with/without irrigation are shown in **Figure C1**.

[1] http://www.fao.org/docrep/x0490e/x0490e0e.htm
[2] Anon. Scheduling overview. NZ Avocado Industry 11 Mar 2010. (accessed 16 Jul 2015) <http://www.hortinfo.co.nz/factsheets/fs110-68.asp>.

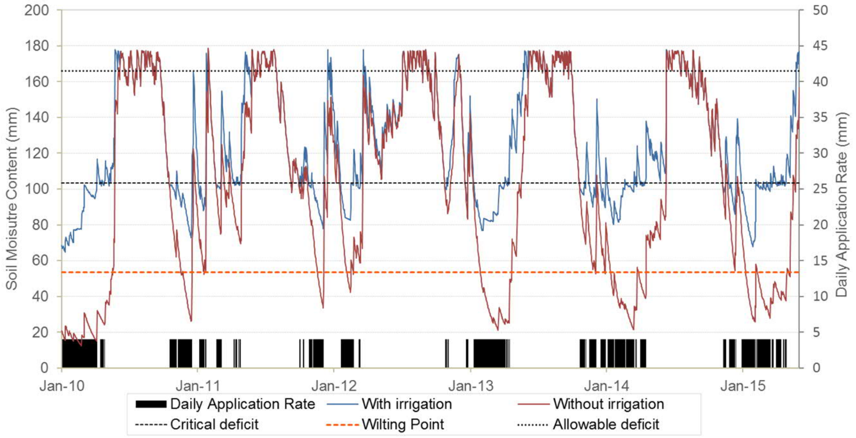

Figure C1. Irrigation simulation output for time period 2010-2015

The daily peak application rate was optimised through a set of simulations, aiming to minimize the water losses through surface runoff and percolation to groundwater system, while maintaining a soil moisture content that is above the plant critical deficit.

The simulations indicate an optimized peak application rate of 4 mm/day. The relationship between annual irrigation amount and peak application rate is shown in **Figure C2**.

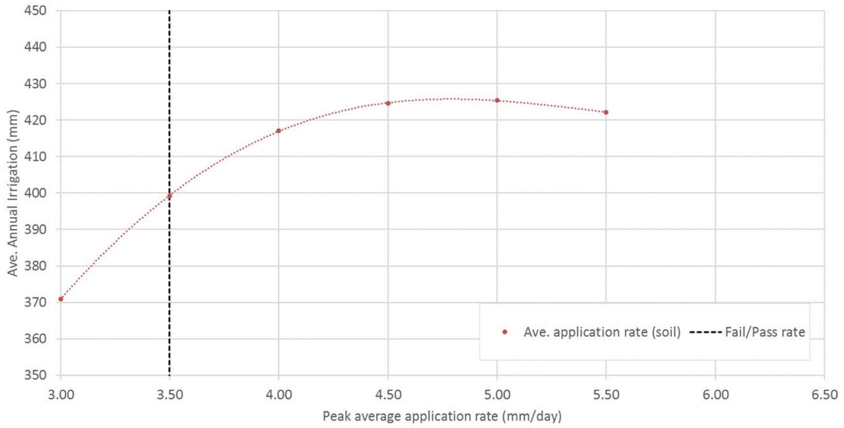

Figure C2. Assessment of peak application rate that is water conservative for sandy soils.

The irrigation demand was simulated for the period of 01/01/1960 to 31/07/2018 and a summary graph showing the number of days irrigation was required per season is shown in **Figure C3**.

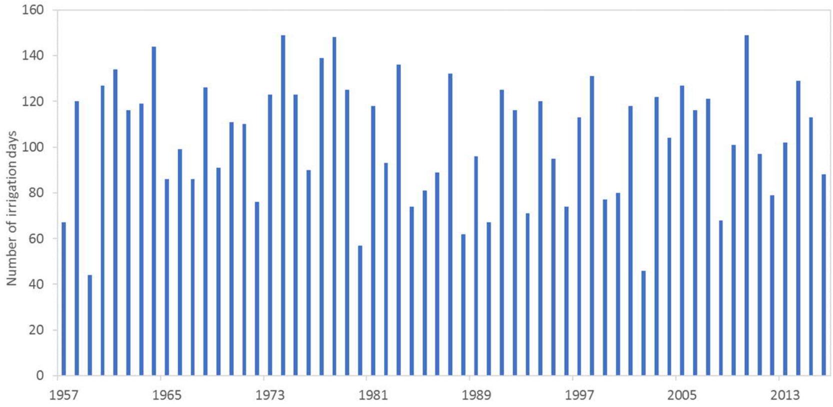

Figure C3. Simulated number of irrigation days per season.

The statistical distribution of monthly irrigation application totals, with 10% additional water added to account for irrigation inefficiency, is shown in **Figure C4**.

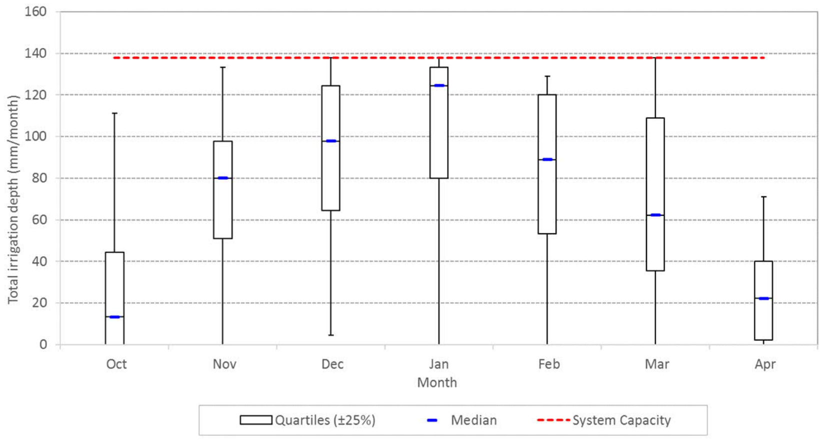

Figure C4. Seasonal irrigation demand for sandy soil.

The annual irrigation demand volume and commensurate number of days of irrigation was calculated and it was found that the 90%ile of simulated annual demand is equivalent to approximately 150 days pumping at the peak rate. This closely aligns with the annual volumes specified in consents granted.

D.2 Development of an irrigation actual use dataset

The simulated irrigation demand time series was applied to one of the currently consented groundwater bores with a peak allocation rate of 720 m^3/day owned by Ivan Stanisich (NRC consent No. CON20102739101). The total amount of demand simulated during the irrigation period was calculated and compared with available historical use records, as shown in **Figure C5**.

The simulated demand varies with climate conditions from a minimum of 44 days irrigation to a maximum of 149 days irrigation during the irrigation season. For the years where records were available for comparison, measured demand is approximately 30% of simulated demand. There are a number of minor reasons for this including human operational decision and actual rainfall not being totally consistent with site rainfall, but the primarily reason is that the orchard is not fully developed.

Considering the scope and purpose of this modelling, this irrigation demand time series is a conservative estimate and therefore appropriate to use in effects assessment from the abstraction of groundwater.

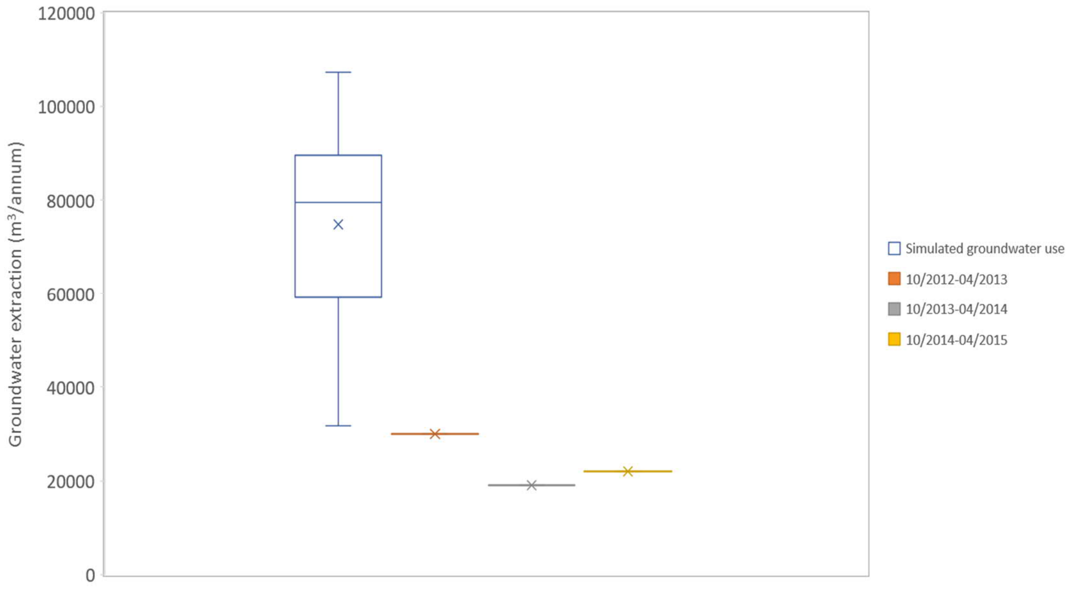

Figure C5. Comparison between the simulated groundwater demand and the historical records.

The irrigation demand pattern from **Section C.1** was applied to all the groundwater irrigation bores in the model area to construct transient pumping time series input for the model.

Appendix E. Calibrated Model Hydrographs

Waterfront (19 m)

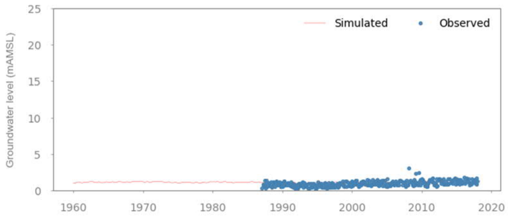

Waterfront (37 m)

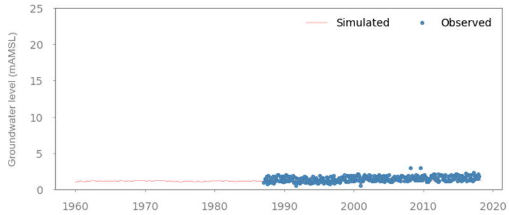

Waterfront (57 m)

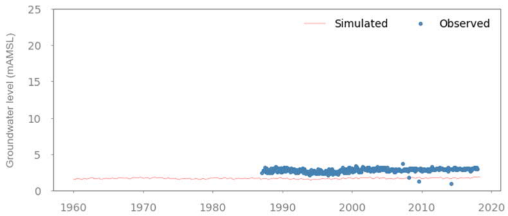

Waterfront (74 m)

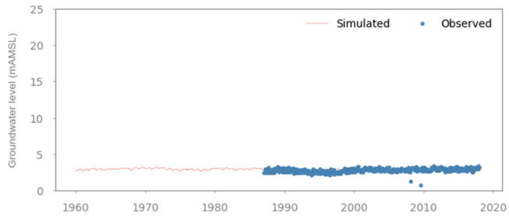

Fishing Club (78 m)

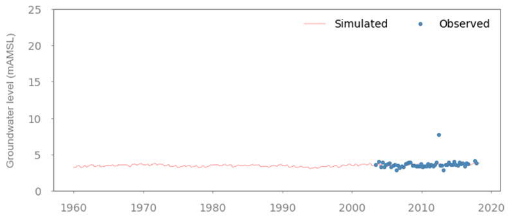

Wagener (69 m)

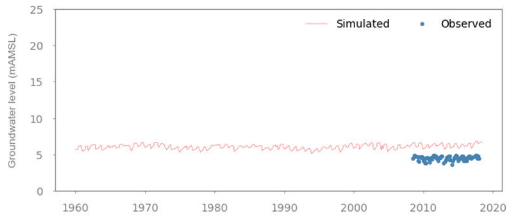

Browne (16 m)

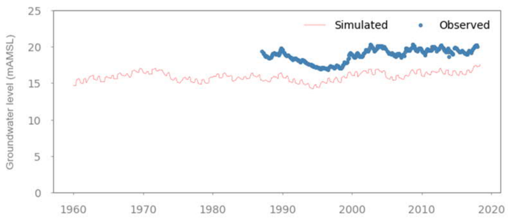

Browne (29 m)

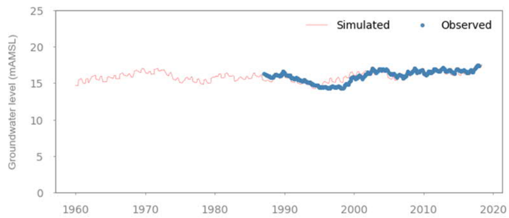

Browne (59 m)

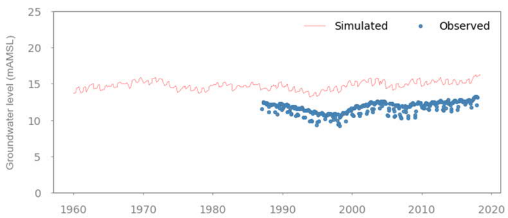

Forest (16 m)

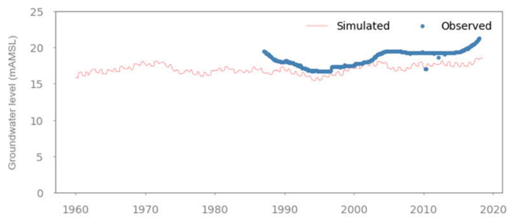

Forest (36 m)

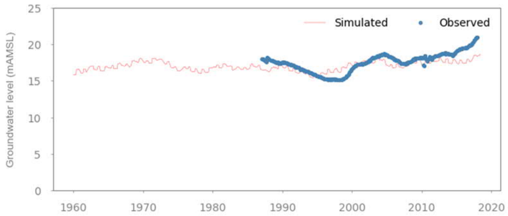

Forest (64 m)

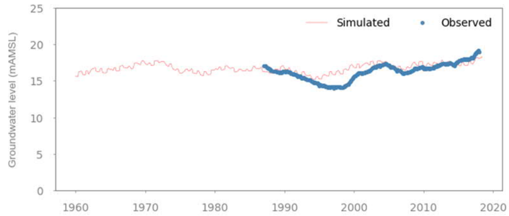

Forest (79 m)

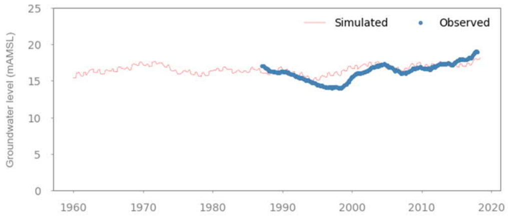

Hukatere (19 m)

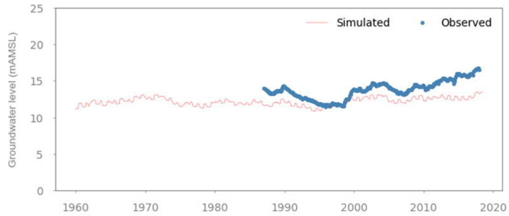

Hukatere (36 m)

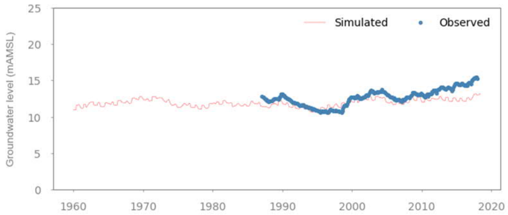

Hukatere (58 m)

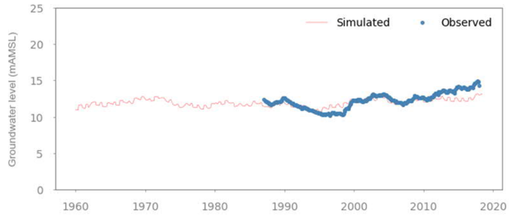

Kaimaumau Deep (72 m)

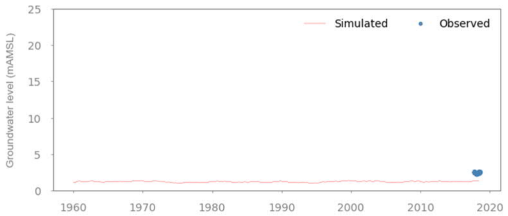

Paparore (18 m)

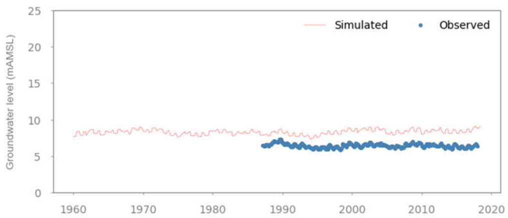

Paparore (35 m)

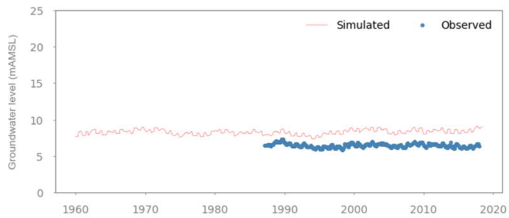

Paparore (65 m)

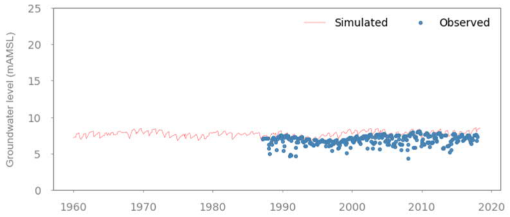

Paparore (75 m)

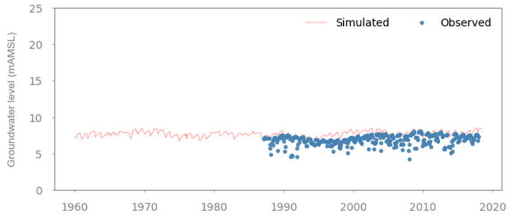

Ogle Drive (68 m)

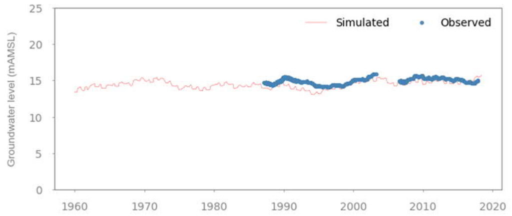

Valic-1 (Shallow Monitoring-17 m)

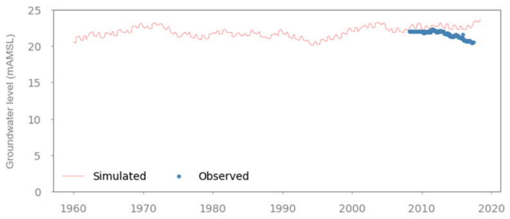

Valic-1 (Deep Monitoring-103 m)

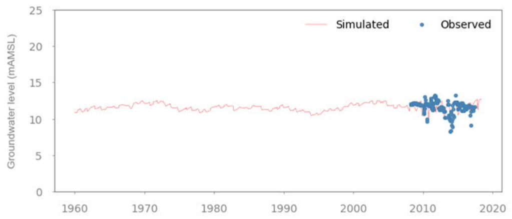

Valic-1 (Production Bore-103 m)

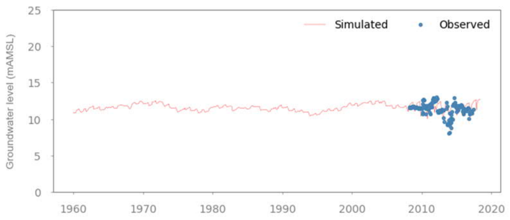

Valic-2 (Shallow Monitoring-55 m)

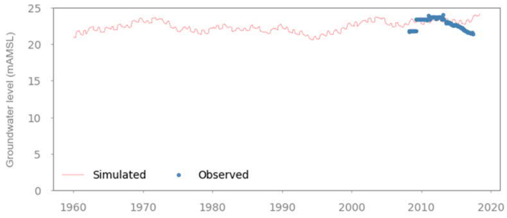

Valic-2 (Deep Monitoring-121 m)

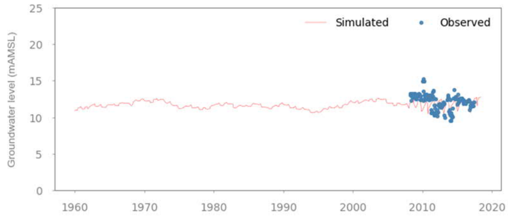

Valic-2 (Deep Production-121 m)

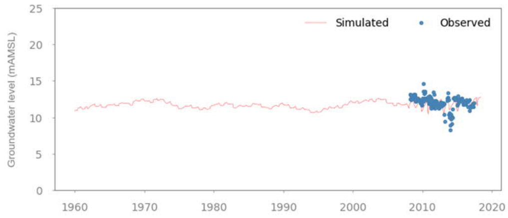

Valic-3 (Shallow Monitoring-45 m)

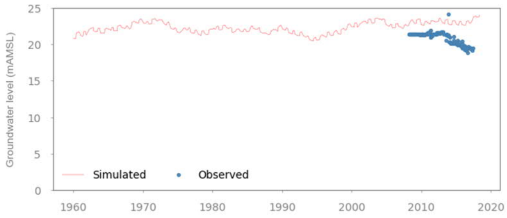

Valic-3 (Deep Monitoring-124 m)

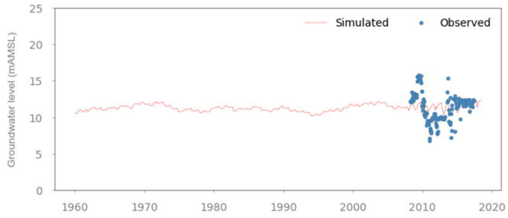

Valic-3 (Deep Production-124 m)

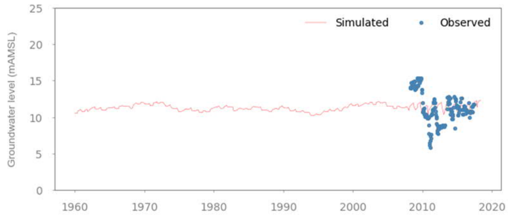

Valic-4 (Shallow Monitoring-13 m)

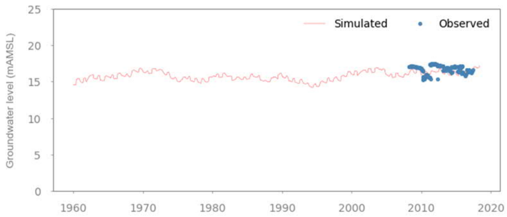

Valic-4 (Deep Monitoring-93 m)

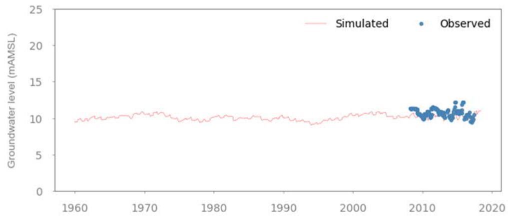

Valic-4 (Deep Production-93 m)

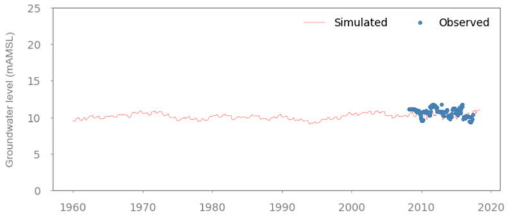

Sweetwater MW1 (13 m)

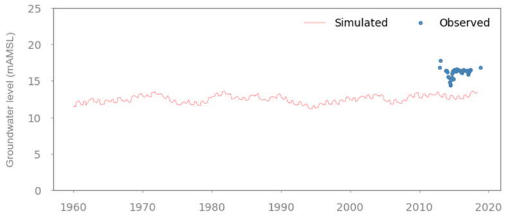

Sweetwater MW1 (94 m)

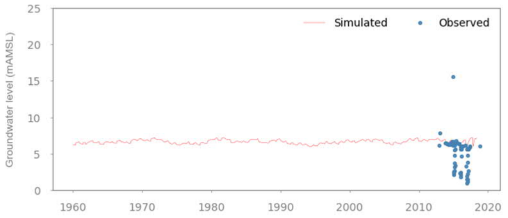

Sweetwater MW2 (15 m)

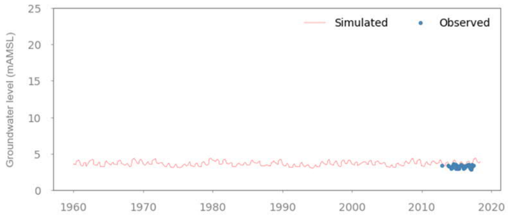

Sweetwater MW2 (59 m)

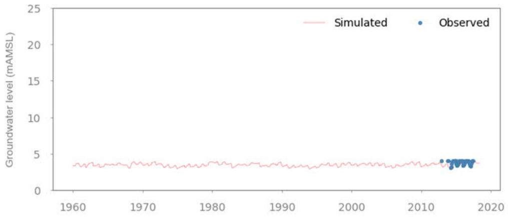

Sweetwater MW3 (5 m)

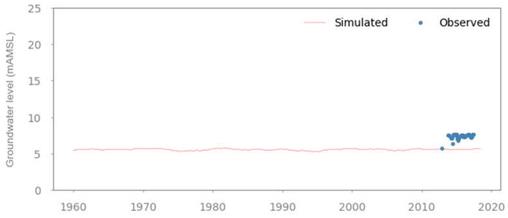

Sweetwater MW3 (47 m)

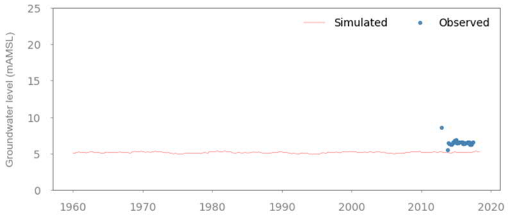

Sweetwater MW4 (25 m)

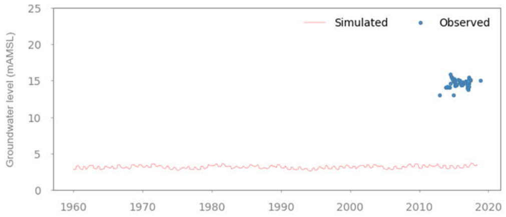

Sweetwater MW4 (92 m)

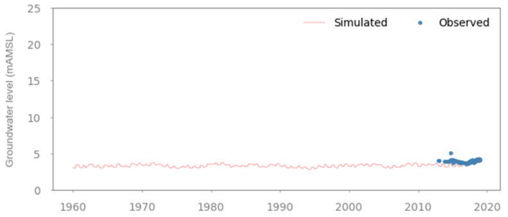

Sweetwater MW5 (6 m)

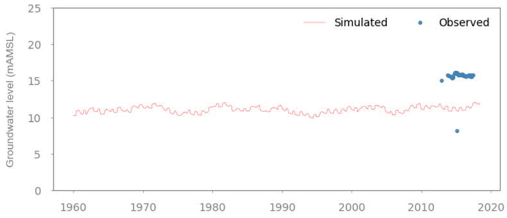

Sweetwater MW5 (61 m)

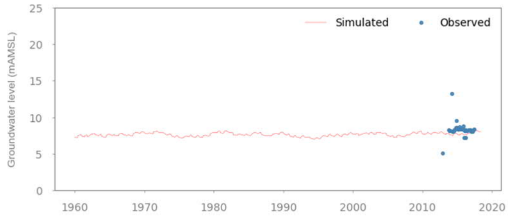

Sweetwater MW6 (15 m)

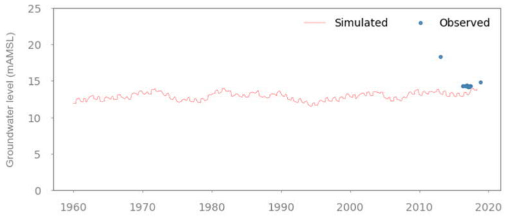

Sweetwater Nursery (34 m)

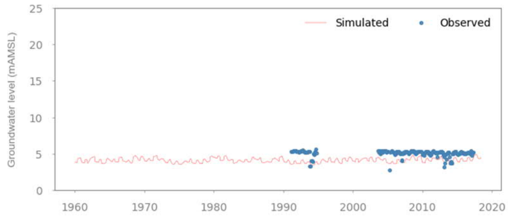

Waipapa (56 m)

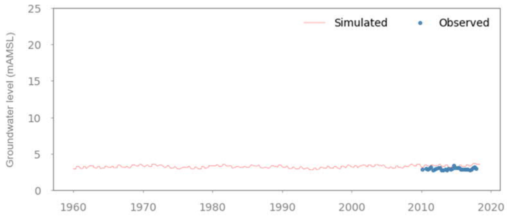

Shanks (Unknown depth)

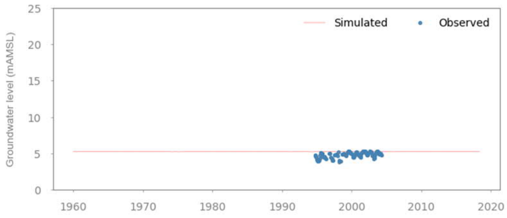

Vinac (33 m)

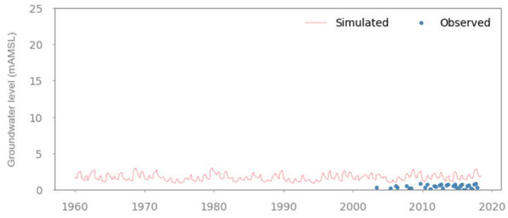

Matich (Unknown depth)

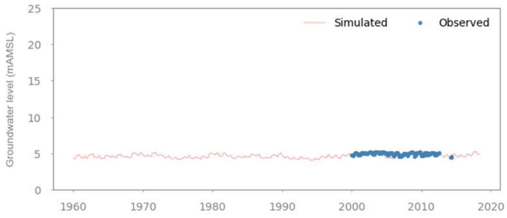

Welch (32 m)

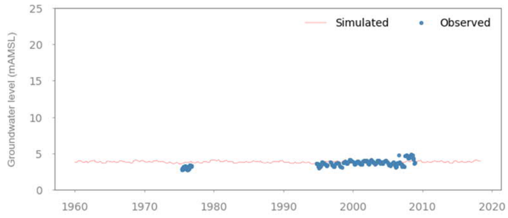

Lake Heather 1 (26 m)

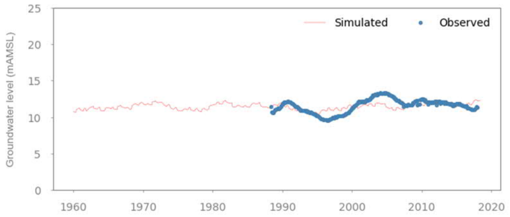

Lake Heather 1 (105 m)

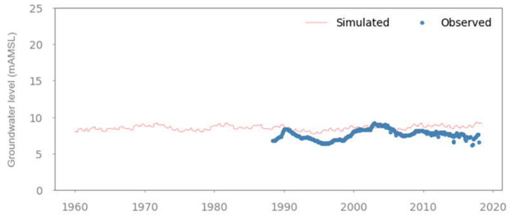

Lake Heather 2 (29 m)

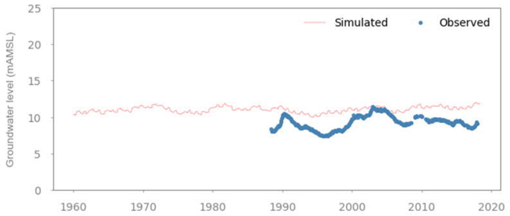

Lake Heather 3 (29 m)

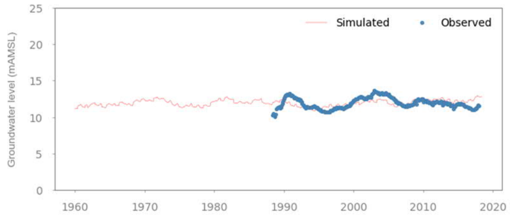

Figure E1. Hydrographs of simulated versus observed groundwater levels.